# Nonadiabaticity and large fluctuations in a many-particle Landau-Zener problem

Alexander Altland,[1] V. Gurarie,[2] T. Kriecherbauer,[3] and A. Polkovnikov[4]
[1]*Institut für Theoretische Physik, Zülpicher Str. 77, 50937 Köln, Germany*
[2]*Department of Physics, CB390, University of Colorado, Boulder, Colorado 80309, USA*
[3]*Fakultät für Mathematik, Ruhr-Universität Bochum 44780, Bochum, Germany*
[4]*Department of Physics, Boston University, Boston, Massachusetts 02215, USA*
(Received 4 December 2008; published 2 April 2009)

We consider the behavior of an interacting many-particle system under slow external driving—a many-body generalization of the Landau-Zener paradigm. We find that a conspiracy of interactions and driving leads to physics profoundly different from that of the single-particle limit: for practically all values of the driving rate the particle distributions in Hilbert space are very broad, a phenomenon caused by a strong amplification of quantum fluctuations in the driving process. These fluctuations are "nonadiabatic" in that even at very slow driving it is exceedingly difficult to push the center of the distribution toward the limit of full ground-state occupancy. We obtain these results by a number of complementary theoretical approaches, including diagrammatic perturbation theory, semiclassical analysis, and exact diagonalization.

DOI: 10.1103/PhysRevA.79.042703 PACS number(s): 03.65.Nk, 03.65.Sq, 03.65.Yz, 05.45.Mt

## I. INTRODUCTION

In many physical contexts, one is met with quantum systems that are subjected to "slow" time-dependent external driving. The most elementary prototype in this category, the Landau-Zener (LZ) system [1,2], contains just two coupled levels driven linearly in time. In this system, the initially occupied instantaneous ground-state level of its Hamiltonian

$$\hat{H} = \begin{pmatrix} \lambda t & g \\ g & -\lambda t \end{pmatrix} \tag{1}$$

stays occupied in the infinite future with a probability

$$P = 1 - e^{-\pi g^2/\lambda}, \tag{2}$$

where $g$ is the coupling strength, $\lambda$ defines the driving rate and $\exp(\pi g^2/\lambda)$ is the so-called Landau-Zener parameter. The approach $P \underset{\lambda\to 0}{\to} 1$ is manifestation of the quantum adiabatic theorem, i.e., the statement that sufficiently slow driving keeps a quantum system in its adiabatic ground state.

Many quantum single-particle systems can be effectively described in terms of the Landau-Zener setup or one of its multidimensional generalizations [3–6]. The reason is that the driven approach of pairs of instantaneous eigenstates will generate "avoided crossings" which can be represented by Hamiltonians such as in Eq. (1). The cumulative statistics of these crossings then describes the behavior of the system in the course of the driving process. In particular, the system will remain in its ground state if only the latter is sufficiently well separated from the first excited states.

But how do many-particle systems behave under driving? Given the exponential abundance of energy levels in interacting systems (or the fact that superimposed on the ground state we often have a continuum of low-lying "soft" excitations) reference to the adiabatic theorem will not be sufficient to understand the consequences of driving. In some instances, it is possible to reduce the problem to one of studying the statistics of linear (oscillator) excitations superimposed on an invariant ground state. A system of this type has been studied in work by Yurovsky *et al.* [7] (see also [8]), with the principal observation that the driving process generates a number of $x$ excitations, where

$$x \equiv \exp(\pi g^2/\lambda) \tag{3}$$

coincides with the Landau-Zener parameter.

In general, however, many-particle systems cannot be linearized. The ramifications of nonlinearities in a driven context have been studied in Refs. [9–11], within the simplifying framework of a low-dimensional system (specifically, a Bose-condensed system which can be described in terms of a single complex condensate amplitude.) Describing its dynamics in terms of a nonlinear Schrödinger equation, Refs. [10,11] observed examples of rather interesting behavior, including situations where the system does not remain in the ground state even in the fully adiabatic limit. The problem is also particular in that it has a low-dimensional Hilbert space.

References [12,13] considered an interacting driven system which is generic in that it shows the two principal characteristics of interacting quantum systems: a high-dimensional Hilbert space and nonlinearity. In one of its representations, the system describes a large assembly of degenerate fermions which may pair combine into a bosonic level as their energy gets pushed up (a cartoon of a fermion/boson conversion process as realized in, say, a time-dependent Bose-Einstein condensate (BEC) Bardeen-Cooper-Schrieffer (BCS) superconductor crossover. Quite strikingly, it turned out that this system resists getting close to its adiabatic ground state, i.e., a state where all particles eventually have become bosonic; even at very slow driving an $O(1)$ fraction of particles remains in energetically high-lying sectors of Hilbert space. In fact, the methods employed in Ref. [12] did not enable us to get close to the "adiabatic regime" of the model. The approach to adiabaticity was discussed in Ref. [13] by mapping the evolution of the system to an effective Hamiltonian dynamical system. In this way, as we show in this paper, the exponential dependence (2) gives way to a power law

 

$$1-\frac{n_b}{N}\sim\lambda$$

controlling the ground-state occupancy for a wide range of initial conditions. Here $n_b\in[0,N]$ is the number of particles in the bosonic ground state and $N$ is the total number of particles. Formally, the reluctance of the system to approach its ground state may be understood in terms of dynamical instabilities [13] (to be discussed in some details further below.) Physically, it reflects the general inertia of interacting systems to adjust to (time-dependent) environmental changes.

In this paper, we will discuss an interaction phenomenon which is no less remarkable: the slow dynamical evolution of the system goes along with an exceptionally strong buildup of quantum fluctuations: although we are dealing with a system that should behave "semiclassically," on account of the largeness of its number of particles, $N$, the distributions of particles in Hilbert space turn out to be very broad. This phenomenon can be attributed to an amplification of quantum fluctuations: classically, the driving process changes the relative energy of two many-particle systems. At some point, the originally lower (stable) system becomes higher in energy (unstable). In a strict classical sense, however, the ground state of the elevated system remains stationary. It takes the action of weak $[O(N^{-1})]$ quantum fluctuations to destabilize this state and initiate the evolution toward energetically more favorable sectors of Hilbert space. The nonlinearity of that evolution (interactions) then leads to an amplification of the initial fluctuations, up to a point where they become of $O(1)$. Specifically, we find that

(i) in all but the extreme adiabatic limit $N-n_b\ll N$ the ground-state occupation $n_b$ shows massive fluctuations, $\mathrm{var}(n_b)/\langle n_b\rangle^2=O(1)$. At intermediate mean occupancy $\langle n_b\rangle\simeq N/2$, the distribution $P(n_b)$ extends over almost the full interval $[0,N]$ and

(ii) at fast rates $n_b\ll N$, the probability distribution is exponential: $P(n_b)\propto\exp[-n_b/\langle n_b\rangle]$. At slower rates, it becomes even broader and covers Hilbert space in a manner for which we have no analytical expressions. At yet slower rates, upon approaching the adiabatic limit, the distribution gets 'squeezed' into the boundary region $n_b/N\sim 1$. It then assumes a universal Gumbel form [14], with the latter frequently appearing in the context of extreme value statistics.

In this paper, we will set the stage for the discussion of fluctuations by establishing contact between our earlier "quantum" approach to the problem—the latter adjusted to regimes of fast and moderate driving—and a slow driving semiclassical formulation. Our semiclassical approach is different from that of Ref. [13] in that it microscopically connects to the early quantum stages of the evolution, a matching procedure necessary to explore the role of fluctuations.

The rest of the paper is organized as follows. In Sec. II we will present the spin variant of the model and discuss the mapping to its other representations. We will then analyze the system, in a manner that is structured according to the driving rate. In Sec. III we discuss the regime of moderately high driving rates, where the system can be effectively linearized and admits a full analytical solution. In Sec. IV we go beyond the linear regime and consider driving rates $1<\lambda^{-1}<O(\ln N)$ in terms of effective rate equations. Although these equations become uncontrolled for values $\lambda^{-1}\sim O(\ln N)$, they are good enough to signal the system's reluctance to approach the adiabatic limit. In Sec. V we will formulate the semiclassical approach to the model and the so-called truncated Wigner approximation (TWA). This approximation becomes highly accurate at sufficiently large $N\gtrsim 10$ and for all values of the driving rate. In Sec. VI we use the method of adiabatic invariants to explore the semiclassical theory at very slow driving, $\lambda^{-1}=O(\ln N)$. In Sec. VII, the quality of the results obtained in this way will be checked by comparison to direct numerical solutions of the Schrödinger equation of our problem [which is feasible for particle numbers up to $N=O(10^3)$] and to the simulations of the semiclassical approximation (the latter extensible to much larger $N$). We will also compare to previous work in the literature. In Sec. VIII we discuss a number of ramifications of our problem relating to previous theoretical and experimental works. We conclude in Sec. IX.

## II. MODEL

In this section we will present the theoretical model discussed in most of the rest of the paper—a high-dimensional generalization of the spin-boson model. We will also present a number of less abstract equivalent representations, some resonant with concrete experimental activity.

### A. Definition of the model

Consider an SU(2) spin of value $S=N/2\gg 1$ coupled to a time varying magnetic field of strength $(-\lambda t)$ in the $z$ direction. This will be the first quantum system participating in the driving process. Its partner system is a single bosonic mode at energy $(-\lambda t)$. We couple these two compounds by declaring that the creation of a boson goes along with a lowering of the spin by 1. The total system is then described by the Hamiltonian

$$\hat{H}=-\lambda t b^\dagger b+\lambda t S^z+\frac{g}{\sqrt{N}}(b^\dagger S^-+bS^+),\tag{4}$$

where $g/\sqrt{N}$ defines the coupling strength and $S^\pm=S_x\pm iS_y$. The Hamiltonian (4) obeys the conservation law $[\hat{H},S^z+b^\dagger b]=0$, showing that the total Hilbert-space dimensionality of the problem is $2S+1=N+1$. The linear growth of the dimension of Hilbert space in $N$ is of course not representative for "generic" interacting systems (dimensionality exponential in $N$). An increase in the dimensionality of the problem can be effected by symmetry breaking, e.g., by replacement of the large spin by an assembly of $N$ nondegenerate spin-1/2 compounds (cf. discussion in Sec. II C below). While this generalization will make the problem largely intractable, we believe it to have little qualitative effect, as long as the band splitting is smaller than the hybridization strength with the boson mode.

Below it will be useful to think of $b$ as a transverse magnetic field acting on the spin. The above conservation then implies that the transverse field strength is proportional to the

deviation of the spin off total polarization $S_z=S$. This feedback mechanism of the spin precession into the field strength encapsulates the effect of interactions in the spin variant of our model. However, before proceeding, let us present a few alternate representations which make the interpretation of the model as one of interacting particles more transparent (cf. Fig. 2):

(1) The variant dominantly discussed in earlier work describes the hybridization of energetically degenerate pairs of spinful fermions with a boson mode [cf. the Hamiltonian (7) below]. This may be viewed as a dispersionless approximation of the fermion-boson conversion processes realized in BEC/BCS crossover experiments in fermionic condensates [15,16] [cf. Fig. 2(b)]. [Although the initial full occupancy of the flat fermion band assumed in [12] may not be adequate to the description of the experimental situation [17] (see Sec. VIII below.)]

(2) Identifying the empty (doubly occupied) configurations of the fermion levels with the two states of a spin 1/2, the system maps onto a time-dependent variant of the Dicke model [18]. In this form it is relevant to the description of super-radiance phenomena in molecular magnetism [19] and to cavity QED with many two-level systems [20].

(3) In a somewhat less obvious representation, the model describes the conversion of pairs of bosons into dimers. In this incarnation it is of relevance to recent experimental work of the JILA group. In these experiments, identical [21] or different [22] species of atoms undergo sweep through a Feshbach resonance to form diatomic molecules. (On the level of effective classical equations of motions, this correspondence was noted in earlier references [13]. Below, we will establish the connection within a fully quantum-mechanical setting.)

For the convenience of interested readers, the equivalence between these different incarnations of the model is established in Sec. II C below. While the "spin-boson" formulation (4) does not relate to concrete physical systems in an obvious way, we find it ideally suited to our theoretical analysis and much of our later discussion will be formulated in this language. However, it is straightforward to transcribe all conclusions to the context of the other models.

### B. Formulation of the problem

The problem we will address in most of the paper is formulated as follows. Start the dynamics in the distant past in the adiabatic ground state of the problem: spin fully polarized $S_z=S=N/2$ and zero bosons $n_b(t)\equiv\langle b^\dagger(t)b(t)\rangle=0$. The goal is to find the number of produced bosons at large positive times,

$$n_b \equiv \lim_{t\to\infty} n_b(t) \equiv \lim_{t\to\infty}\langle b^\dagger(t)b(t)\rangle. \tag{5}$$

The adiabatic limit is reached when $n_b\to N$ or, equivalently, $S_z=-S$. Alternatively, we can speak of the representation in terms of bosonic atoms and bosonic molecules, given by Eqs. (8) and (10), where this initial condition implies the absence of atoms in the distant past, and the goal is to find the number of produced atoms at large positive times.

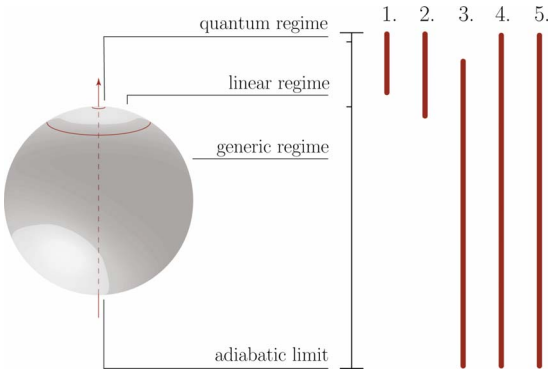


FIG. 1. (Color online) Different theoretical approaches to the problem. The Hilbert space of the problem contains a number of different sectors: a (quantum fluctuation) dominated region where only a few bosons have been created $n_b=O(1)$ and the spin remains nearly polarized, a "linear region," where the number of bosons may be large but is small enough to justify linearization of spin operators, $1\ll n_b\ll N$, a generic region, $n_b=O(N)$, and the adiabatic limit $n_b\to N$. Theoretical approaches we will use to approach these regimes include (1) solution of the linearized Schrödinger equation (cf. Sec. III), (2) Keldysh perturbation theory based on a self-consistent RPA approximation (cf. Sec. IV), (3) semiclassical approach based on the approximate conservation of adiabatic invariants (cf. Sec. VI), (4) an extended semiclassical scheme, where semiclassical methods are employed to propagate the full quantum distribution beyond the quantum regime (cf. Secs. V and VII), and (5) numerical solution of the Schrödinger equation for moderately large $N$.

As was anticipated in Sec. I, the operator $b^\dagger b$ exhibits strong quantum fluctuations. It will, thus, be of interest to explore the *distribution* $P(n)$ defined by the moments $\langle(b^\dagger b)^k\rangle$. Also, there may be physical situations where it is not appropriate to start the process in the spin-up polarized state. We have already mentioned the case of dilute fermion gases [17] where a near south polar configuration may be a more appropriate starting point. Similarly, a downward polarized state $S_z=-S$ (in an initially downward pointing field) will model an atom→molecule conversion process with a purely atomic starting configuration.

In the following, we will describe different stages of the conversion process, where the organizing principle will be the conversion efficiency, which in turn depends on the speed of the sweeping process. For later reference, the different parameter regimes, along with the theoretical methods we will use to describe them, are summarized in Fig. 1.

### C. Alternate model representations

The equivalence to a system of boson-coupled degenerate two-level systems—the *time-dependent Dicke model*—is best seen starting from the latter. Consider the Hamiltonian

$$\hat{H} = -\lambda t b^\dagger b + \frac{\lambda t}{2}\sum_{i=1}^{N}\sigma_i^z + \frac{g}{\sqrt{N}}\sum_{i=1}^{N}(b^\dagger\sigma_i^- + b\sigma_i^+), \tag{6}$$

where $\sigma^{x,y,z}$ are Pauli matrices acting in pseudospin space. The fact that the spin operators appear in totally symmetric

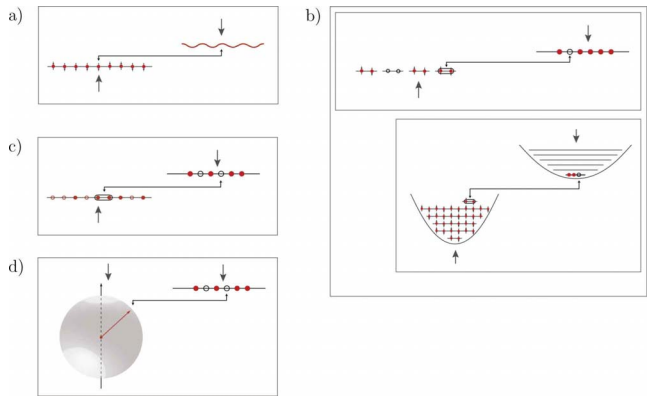


FIG. 2. (Color online) The different incarnations of the model: (a) time-dependent Dicke model: an assembly of degenerate two-level systems coupled to a boson mode, (b) flat-band approximation (top) to a system of spinful fermions pair binding into bosonic molecules, (c) system of atoms pair converting into molecules, and (d) spin subject to a magnetic field and coupled to a bosonic level.

combinations $\Sigma_i \sigma^{x,y,z}$ suggests considering the total spin operator $S^{x,y,z} \equiv \frac{1}{2}\Sigma_i \sigma^{x,y,z}$. The operators $S^{x,y,z}$ define an SU(2) algebra. Denoting the maximum weight space "all fermions occupied" by $|S\rangle$, we observe that $S^z$ has maximal eigenvalue $S=N/2, S^z|S\rangle = S|S\rangle$. This shows that the operators $S^{x,y,z}$ act in a Hilbert space of dimension $2S+1=N+1$. The global spin representation of the Hamiltonian (6) is but the starting Hamiltonian (4). The Hamiltonian (6) is represented in Fig. 2(a). As mentioned in Sec. I, a natural experimental realization of Eq. (6) is a cavity QED with $N$ two-level systems.

The *Fermi-Bose crossover model* describes a system of $2N$-degenerate spinful fermion states. Two fermions occupying such a state may combine to form a boson populating one ("condensate") bosonic state. Starting from an infinitely low initial value, the energy of the fermions gets pushed up linearly in time [cf. Fig. 2(b)]. This setup is described by the Hamiltonian

$$\hat{H} = -\lambda t b^\dagger b + \frac{\lambda t}{2}\sum_{i=1}^{N} (a_{i\uparrow}^\dagger a_{i\uparrow} + a_{i\downarrow}^\dagger a_{i\downarrow}) + \frac{g}{\sqrt{N}}\sum_{i=1}^{N} (b^\dagger a_{i\downarrow} a_{i\uparrow} + b a_{i\uparrow}^\dagger a_{i\downarrow}^\dagger), \tag{7}$$

where $\lambda$ is the driving rate, $g/\sqrt{N}$ is the coupling amplitude of the conversion process, and $a_{i,\uparrow\downarrow}$ and $b$ are fermion and boson annihilation operators. For convenience, we have split the time-dependent energy symmetrically between bosons and fermions. (By a gauge transformation any distribution of energies with fixed difference $2\lambda t$ between a boson and a pair of fermions can be realized.)

Noting that the interaction couples only two ($|\uparrow,\downarrow\rangle$ and $|0\rangle$) of four possible ($|\uparrow,\downarrow\rangle$, $|\uparrow\rangle$, $|\downarrow\rangle$, and $|0\rangle$) occupation states of a spinful fermion level, we may consider a pseudospin state to discriminate between these two states $|\uparrow,\downarrow\rangle \leftrightarrow \binom{1}{0}$ and $|0\rangle \leftrightarrow \binom{0}{1}$. The pseudospin representation of the Hamiltonian is but Eq. (6).

We may think of the Hamiltonian (7) as a cartoon version of more realistic models. For example, it can be interpreted as a nondispersive (flat-band) approximation to a system of free fermions coupled to the lowest mode of an electromagnetic field in a cavity QED setup. Alternately, it may be regarded as a cartoon version of a BCS/BEC crossover system wherein a band of (lattice) fermions is initially filled, the band dispersion is neglected, and only the lowest condensate state of the bosons ("molecules") is kept [Fig. 2(b) inset]. While the neglect of dispersion effects may be acceptable [17], the assumption of full band occupancy might not be met in experiment. [Reference [17] argues that the full band assumption should be modeled by starting the dynamics in incompletely "polarized" (pseudo)spin states, and we refer the reader to this work for a discussion of this case.] For completeness, let us mention that the problem of the dynamic BCS/BEC crossover has been addressed in many publications and using different approaches, beginning with [23] and continuing with Refs. [13,17,24–26]. It is probably fair to say that a consensus on whether this problem can indeed be reduced to the flat-band model with a single Bose mode (7) has not yet been reached in the literature.

Finally, consider a system of atoms sweeping through a Feshbach resonance whereafter diatomic molecules form the energetically preferred state (cf. Ref. [21] where the conversion processes has been realized in condensates of $^{85}$Rb or $^{40}$K atoms). This situation is described by the Hamiltonian

$$\hat{H} = \lambda t d^\dagger d - \frac{\lambda t}{2} c^\dagger c + \frac{g}{\sqrt{N}}(d^\dagger c c + d c^\dagger c^\dagger). \tag{8}$$

This Hamiltonian describes the *conversion of atoms to molecules*, where the former or latter are created by the bosonic operators $c^\dagger/d^\dagger$, and the symmetry $[\hat{H}, d^\dagger d + 2c^\dagger c]=0$ reflects the conservation of the total number of particles. The time-independent version of this model was extensively analyzed in Ref. [27].

The (near) equivalence to the previous model representations is seen by computing matrix elements $M_{N,n} \equiv \langle N-n+1, 2n-2|\hat{H}|N-n, 2n\rangle$, where the state $|N-n, 2n\rangle$ contains $(N-n)$ $d$ molecules and $2n$ $c$ atoms. Evaluating the matrix element, we find

$$M_{N,n} = \frac{g}{\sqrt{N}}\sqrt{(N-n+1)n(n-1/2)}.$$

Now, let $|N/2-n, n\rangle'$ be the state with $n$ bosons and spin polarization $S_z = N/2-n$. Computing the matrix elements $M'_{N,n} \equiv \langle N/2-n+1, n-1|\hat{H}|N/2-n, n\rangle$ of the Hamiltonian (4), we find

$$M'_{N,n} = \frac{g}{\sqrt{N}}\sqrt{(N-n+1)n^2}. \tag{9}$$

The matrix elements $M$ and $M'$ are identical up to corrections of $O(n^{-1})$ which vanish in the limit of large particle number occupancies. This consideration shows that the conversion of atoms to molecules can be discussed within the framework of the spin Hamiltonian above, where the number

TABLE I. Survey of the equivalent representations of the model.

| Model | System A | System B |
|---|---|---|
| Spin-boson | Spin $S=N/2$ | Boson mode |
| Time-dependent Dicke model | $N$ two-level systems | Boson mode |
| Fermi-Bose conversion | Flat band of $2N$ fermion states | Boson mode |
| Atom-molecule conversion | Dibosonic molecular state | Boson mode |

of molecules is counted in terms of the spin quantum number.

The correspondence between models can be made perfect by considering heteromolecular conversion processes (cf. Ref. [22] for a realization in an $^{85}$Rb-$^{87}$Rb gas). Straightforward generalization of Eq. (8) obtains the Hamiltonian

$$\hat{H} = \lambda t d^\dagger d - \frac{\lambda t}{2}(c_1^\dagger c_1 + c_2^\dagger c_2) + \frac{g}{\sqrt{N}}(d^\dagger c_1 c_2 + d c_1^\dagger c_2^\dagger), \tag{10}$$

where $c_{1/2}^\dagger$ creates atoms of species 1/2 and $d^\dagger$ the (1-2) heteromolecule. It is not difficult to verify that the matrix elements of this Hamiltonian *exactly* coincide with those of the spin-boson Hamiltonian (4).

In this incarnation our problem has been analyzed by a number of authors. Its classical version constitutes a specific example of more general problems in the theory of nonlinear differential equations studied in Ref. [28]. More recently, it was analyzed by Ref. [7] (see also the more recent Ref. [29]). It is also in this form that the problem is the closest to existing experiments [21,22].

Equations (4) and (6)–(8) define four equivalent definitions of the model. For the convenience of the reader, the correspondence between the systems involved in these definitions is summarized in Table I.

## III. LINEARIZED DIABATIC REGIME

We first consider moderately fast driving rates where only a small fraction of the particles undergo a conversion process. In the language of the spin model this means that at large times the spin will still be stuck close to the north polar regions, $\lim_{t\to\infty}[S-S_z(t)]/S \ll 1$, or $n_b/N \ll 1$. In this regime, the curvature of the SU(2) spin manifold is not yet felt and the problem can be effectively linearized.

This is best done in the Holstein-Primakoff representation of spin operators

$$S^- = c^\dagger (2S - c^\dagger c)^{1/2},$$

$$S^+ = (2S - c^\dagger c)^{1/2} c,$$

$$S^z = S - c^\dagger c, \tag{11}$$

where the algebra of bosonic operators $c$ and $c^\dagger$ defines the Holstein-Primakoff bosons. Substitution of the linearized approximation $S^- = (2S)^{1/2} c^\dagger$, $S^+ = (2S)^{1/2} c$, and $S^z = S - c^\dagger c$ into Eq. (4) generates the quadratic Hamiltonian

$$\hat{H}_{\mathrm{HP}} = -\lambda t (b^\dagger b + c^\dagger c) + g(b^\dagger c^\dagger + cb). \tag{12}$$

To compute the number of bosons created in the linearized evolution, we switch to the Heisenberg representation $b(t) = e^{i\hat{H}t} b e^{-i\hat{H}t}$ and consider the expectation value

$$n_b(t) = \langle b^\dagger(t) b(t) \rangle$$

taken with respect to the vacuum state, $\langle \cdots \rangle \equiv \langle 0 | \cdots | 0 \rangle$ with $b|0\rangle = c|0\rangle = 0$. Alternatively, one can consider a model of bosonic atoms and molecules, in the regime where most of the particles are molecules. In the Hamiltonians (8) and Eq. (10) one may then replace $d \to \sqrt{N}$ to arrive precisely at Eq. (12), which is an appropriate relabeling of operators understood. In Ref. [7] a model equivalent to the linearization above was introduced, and the mean conversion rates of the linearized dynamics were computed (see also Ref. [8]).

The computation of $n_b = \lim_{t\to\infty} n_b(t)$ is reviewed in Appendix A, with the principal result

$$n_b = x - 1. \tag{13}$$

Equation (13) states that the number of converted particles grows linearly in the LZ parameter. Unlike with the standard (two-level) LZ problem, the many-particle system remains parametrically detached from adiabaticity, even for large values of the LZ parameter. However, the linearization underlying the derivation limits the validity of the result to $n_b \ll N$.

The techniques used in Appendix A actually yield the entire (quantum) distribution of the number of produced particles,

$$P(n) = \frac{1}{x}(1 - x^{-1})^n \simeq \frac{e^{-n/x}}{x} \quad (x \gg 1). \tag{14}$$

This distribution is very broad. Its width $(\langle n^2 \rangle - \langle n \rangle^2)^{1/2} \simeq x$ is of the same order as its mean. This is remarkable inasmuch as our system is not subjected to any sources of fluctuations, other than its intrinsic quantum fluctuations. We are met with the unusual situation that quantum fluctuations are of the same order as mean values, in spite of the "semiclassical" largeness of the latter, $\langle n \rangle \simeq x \gg 1$. Similar phenomena have been discussed in the context of dynamical sweeps through quantum phase transition points (cf., e.g., Ref. [30]).

## IV. KINETIC EQUATION

### A. Keldysh formalism

An alternative way of analyzing the problem starts from the boson-fermion representation (7) and analyzing the corresponding kinetic equation [theory strand (b) in Fig. 2]. To formulate this approach, we employ the Keldysh formalism and consider the appropriate Keldysh Green's functions (cf. Ref. [31] for a review of the formalism). Readers not interested in the formalism are invited to proceed directly to the discussion of the main result of this section, the rate Eq. (27).

Within the Keldysh formalism, the fermion subsystem is described by the matrix Green's function

$$G_{\sigma\alpha,\sigma'\alpha'}(t,t') = -i\langle a_{\sigma\alpha}(t)a^{\dagger}_{\sigma'\alpha'}(t')\rangle = \begin{pmatrix} G^R & G^K \\ 0 & G^A \end{pmatrix}_{\sigma\alpha,\sigma'\alpha'}(t,t'),$$

where $\alpha,\alpha'=1,2$ index the two-component Keldysh space (to which the matrix structure in the equation refers) and $\sigma=(i,\uparrow\downarrow)$ is a container index comprising the fermion site and spin index. $G^R$, $G^A$, and $G^K$ stand, respectively, for the advanced, retarded, and the Keldysh Greens' function. The latter is defined by

$$G^K = G^R \circ f - f \circ G^A,$$

where the symbol "$\circ$" defines a temporal convolution

$$(A \circ B)(t,t') \equiv \int dt'' A(t,t'')B(t'',t')$$

and $f \equiv 1-2n_f$ defines the distribution of the fermions. In what follows, it will be convenient to represent the Green's functions of the theory in the Wigner representation,

$$G^K(\tau,\omega) = \int dt\, G^K\left(\tau+\frac{t}{2},\tau-\frac{t}{2}\right)e^{i\omega t}, \tag{15}$$

and similarly for all the other Green's functions. In the absence of interactions, $g=0$, a straightforward calculation obtains the Wigner representation of the free Green's functions as

$$G^R_{0,\sigma\sigma'}(\tau,\omega) = \frac{\delta_{\sigma\sigma'}}{\omega^+ - \lambda t/2},$$

$$G^A_{0,\sigma\sigma'}(\tau,\omega) = \frac{\delta_{\sigma\sigma'}}{\omega^- - \lambda t/2},$$

$$G^K_{0,\sigma\sigma'}(\tau,\omega) = -2\pi\delta_{\sigma\sigma'}f_0(\tau,\lambda t/2)\delta(\omega-\lambda t/2), \tag{16}$$

where $f_0(\tau,\lambda t/2)\equiv f_0(\tau)$ describes the distribution of the full fermion band $f_0(\tau)=1-2n_0(\tau)=-1$. In a similar manner the bosons are described by

$$D(t,t') = -i\langle b_\alpha(t)b^{\dagger}_{\alpha'}(t')\rangle = \begin{pmatrix} D^K & D^R \\ D^A & 0 \end{pmatrix}_{\alpha\alpha'}(t,t'), \tag{17}$$

where

$$D^K = D^R \circ F - F \circ D^A$$

and $F=1+2n_b$, with $n_b$ describing the boson distribution. The Wigner representation of the noninteracting boson Green's functions is given by

$$D^R_0(\tau,\omega) = \frac{1}{\omega^+ + \lambda t},$$

$$D^A_0(\tau,\omega) = \frac{1}{\omega^- + \lambda t},$$

$$D^K_0(\tau,\omega) = -2\pi F_0(\tau,-\lambda t)\delta(\omega+\lambda t), \tag{18}$$

where $F_0(\tau,-\lambda\tau)\equiv F_0(\tau)$ relates to the vanishing boson number of the noninteracting problem as $F_0(\tau)=1+2n_0(\tau)=1$.

In order to calculate the number of produced bosons at the end of the Landau-Zener process, we need to calculate the exact bosonic Keldysh Green's function, in terms of which

$$n_b = \lim_{t\to\infty} n_b(t) = \lim_{t\to\infty}(iG^K(t,t)-1)/2 \simeq \frac{1}{2}\left(\lim_{\tau\to\infty}\int\frac{d\omega}{2\pi}F(\tau,\omega)A_b(\tau,\omega)-1\right), \tag{19}$$

where $A_b=-2\,\mathrm{Im}\,D^R$ is the spectral function of the bosons. For large positive times, the Green's functions become effectively uncoupled, $D^R(\omega)$ asymptotes to the free form (18), and $A_b(\omega)\simeq 2\pi\delta(\omega+\lambda t)$. This means that the number of bosons at the end of the process is given by

$$n_b = \lim_{\tau\to\infty}\frac{F(\tau,-\lambda\tau)-1}{2}. \tag{20}$$

### B. Perturbation theory

First, we can try to calculate the bosonic Green's function perturbatively, in powers of $g$ (which means, in practice, in powers of the dimensionless parameter $g^2/\lambda$). This expansion is valid at fast rate $\lambda$, $g^2/\lambda \ll 1$. The lowest-order correction to the bosonic propagator is depicted in Fig. 3, diagram (a). The calculation of this diagram, although cumbersome, proceeds in a straightforward fashion, giving the result

$$n_b \approx \frac{\pi g^2}{\lambda}. \tag{21}$$

Each vertex of the diagram carries a factor of $g/\sqrt{N}$. However, there are $N$ fermions propagating around the loop, canceling the factor $1/N$ coming from the vertices. This results in the cancellation of factors of $N$ in the answer.

In the next order of perturbation theory two more diagrams contribute to the bosonic propagator. These are shown on Fig. 3, diagrams (c) and (d). This leads to the second-order answer

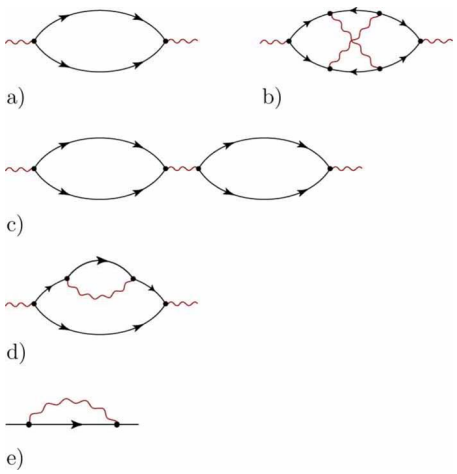


FIG. 3. (Color online) (a)–(e) The lowest-order corrections to the bosonic propagator.

$$n_b \approx \frac{\pi g^2}{\lambda} + \left(\frac{1}{2} - \frac{1}{N}\right)\left(\frac{\pi g^2}{\lambda}\right)^2. \tag{22}$$

Note that at $N=1$, this indeed coincides with the Taylor expansion of the exact Landau-Zener formula

$$n_b = 1 - e^{-\pi g^2/\lambda}. \tag{23}$$

Notice also that at $N>1$, the number of produced particles is larger than at $N=1$. This is natural, as with larger $N$ one can produce more bosons.

Finally, we note that the calculation leading to Eq. (22) closely parallels that employed in Ref. [25] to calculate the molecule production in a Feshbach resonance experiment perturbatively.

### C. Self-consistent random-phase approximation and kinetic equation

Our aim now is to calculate the number of produced bosons in the large-$N$ limit, with all other parameters including $g$ and $\lambda$ kept fixed. Our starting point is the system of kinetic equations (the Wigner transforms of the Dyson equations, cf. Ref. [31]) for the boson and fermion distribution function,

$$(\partial_\tau - \lambda\partial_\omega)F(\tau,\omega) = i(\Sigma^K - (\Sigma^R \circ F - F \circ \Sigma^A))(\tau,\omega), \tag{24}$$

$$\left(\partial_\tau + \frac{\lambda}{2}\partial_\epsilon\right)f(\tau,\epsilon) = i(\sigma^K - (\sigma^R \circ f - f \circ \sigma^A))(\tau,\epsilon). \tag{25}$$

The first of these equations is obtained by evaluating the Wigner transform of the general kinetic equation of a boson system [31] $(-i\partial_\tau + [\hat{H},])F = \Sigma^K - (\Sigma^R \circ F - F \circ \Sigma^A)$ for the Hamiltonian $\hat{H} = -\lambda t$. The second equation is its fermionic analog.

In the "collision integrals" of Eq. (24), $\Sigma^{K,R,A}$ ($\sigma^{K,R,A}$) are the components of the bosonic (fermionic) self-energies. It is not difficult to see that the dominant contributions to these self-energies are given by the diagrams in Figs. 3(a) and 3(e), with external legs truncated. Unlike with the lowest-order perturbation theory discussed above, the fermionic and bosonic propagators appearing in these diagrams are to be understood as dressed propagators, containing self-energy insertions by themselves. [Technically speaking, this means that we will evaluate the self-energies in a self-consistent random-phase approximation (RPA) approximation.] Self-energy diagrams with crossing interaction lines, such as Fig. 3(b), carry factors of $N^{-1}$ relative to the self-consistent RPA diagrams. (See, however, the discussion in the end of this section.)

The derivation of the self-energies for the boson-fermion interaction follows standard procedures [31] and we will not repeat it here. As a result we obtain the equations

$$\begin{aligned}(\partial_\tau - \lambda\partial_\omega)F(\omega) = \frac{g^2}{2}\int \frac{d\epsilon}{2\pi} A\left(\omega - \epsilon - \frac{\lambda\tau}{2}\right)A\left(\epsilon - \frac{\lambda\tau}{2}\right)\{1 \\ + f(\omega-\epsilon)f(\epsilon) - [f(\epsilon) + f(\omega-\epsilon)]F(\omega)\},\end{aligned}$$

$$\begin{aligned}\left(\partial_\tau + \frac{\lambda}{2}\partial_\epsilon\right)f(\epsilon) = \frac{g^2}{2N}\int \frac{d\omega}{2\pi} A\left(\omega - \epsilon - \frac{\lambda\tau}{2}\right)A_b(\omega + \lambda\tau)\{1 \\ + f(\omega-\epsilon)f(\epsilon) - [f(\epsilon) + f(\omega-\epsilon)]F(\omega)\},\end{aligned} \tag{26}$$

where we suppressed the explicit $\tau$ dependencies for notational clarity and $A=-2\,\mathrm{Im}\,G^R$ and $A_b=-2\,\mathrm{Im}\,D^R$ are the spectral functions of the fermions and the boson, respectively. Notice the factor of $N^{-1}$ multiplying the collision integral of the fermions. The absence of this factor in the boson collision integral signals that the boson interacts with all $N$ fermions simultaneously. In contrast, each fermion interacts only with a single boson, which means that the fermionic self-energies carry the uncompensated squared coupling constant $g^2/N$.

Equation (26) defines a particle number conserving system. Consider the quantity $N(\tau) \equiv n_b(\tau) + N n_f(\tau)$. Using Eq. (19) and its fermionic analog $n_f(\tau) = -\frac{1}{2}(\int \frac{d\epsilon}{2\pi} f(\tau,\epsilon)A(\tau,\epsilon) - 1)$, we obtain that the number of particles varies in self-consistent RPA as

$$\frac{dN}{d\tau} = \frac{1}{2}d_\tau\left(\int \frac{d\omega}{2\pi}F(\tau,\omega)A_b(\tau,\omega) - N\int \frac{d\epsilon}{2\pi}f(\tau,\epsilon)A(\tau,\epsilon)\right).$$

Integrating the first (second) Eq. (26) over $\int \frac{d\omega}{2\pi}A_b(\tau,\omega)$ $(\int \frac{d\epsilon}{2\pi}A(\tau,\epsilon))$ and using $\lambda\partial_\omega A_b = \partial_\tau A_b$, we find that the two integrals cancel out and $d_\tau N = 0$.

This is about as far as we will get without further approximations. Below we will argue that the validity of the RPA approximation is limited by the condition $n_b \ll N$. In the limit $n_b/N \to 0$, the self-energies $\sigma^{R/A}$ broadening the energy dependence of the spectral functions become vanishingly small. (The detailed dependence of the broadening depends on the value of time $\tau$.) Relying on this limiting behavior, we will approximate the spectral functions by $A(\epsilon) \simeq 2\pi\delta(\epsilon)$ by $\delta$ functions. This is a bold approximation inasmuch as the

pairs of $\delta$ functions in Eq. (26) enforce the resonance condition $\tau=0$. However, it is this "resonant" time window $\tau\simeq 0$, where the distribution functions entering the integral kernel are expected to vary strongest. This means that the value of the collision integral may well be sensitive to the detailed temporal profile of the distribution functions around $\tau=0$. Ultimately, we will need to compare to the result of other methods to verify the validity of the $\delta$-function approximation.

We substitute the approximations $A_b(\tau,\omega)\simeq 2\pi\delta(\omega+\lambda\tau)$ and $A(\tau,\epsilon)\simeq 2\pi\delta(\epsilon-\lambda\tau/2)$ into Eq. (26), use $n_b(\tau)=\frac{1}{2}[\int\frac{d\omega}{2\pi}F(\tau,\omega)A_b(\tau,\omega)-1]\simeq[F(\tau,-\lambda\tau)-1]/2$, and differentiate with respect to time to obtain

$$\partial_\tau n_b=-\partial_\tau n_f=\frac{\pi g^2}{\lambda}\delta(\tau)[n_f^2+n_b(2n_f-1)]. \tag{27}$$

The meaning of this equation becomes transparent upon rewriting the combination of distribution functions on its right-hand side (r.h.s.) as $(1+n_b)n_f^2-n_b(1-n_f)^2$. This factor weighs the probability that two fermions convert into bosons and back. To solve the equation, we take advantage of the conservation law

$$n_b+Nn_f=N. \tag{28}$$

It is then straightforward to obtain the solution

$$n_b(\tau)=\frac{2N(e^{\sqrt{(N+4)/N}(\pi g^2/\lambda)\theta(\tau)}-1)}{e^{\sqrt{(N+4)/N}(\pi g^2/\lambda)\theta(\tau)}[-N+\sqrt{N(N+4)}+2]+N+\sqrt{N(N+4)}-2}. \tag{29}$$

The singular behavior of $n_b$ at $\tau=0$ is a remnant of the above $\delta$-function approximation. Incidentally, we note that the Taylor series expansion of $n_b$ with respect to $g^2$ gives

$$n_b=\lim_{\tau\to\infty}n_b(\tau)=\frac{\pi g^2}{\lambda}+\left(\frac{1}{2}-\frac{1}{N}\right)\left(\frac{\pi g^2}{\lambda}\right)^2+\frac{6-8N+N^2}{6N^2}\left(\frac{\pi g^2}{\lambda}\right)^3+\cdots. \tag{30}$$

The first two terms indeed match the direct perturbative expansion given by Eq. (22), confirming that this technique does take into account all the diagrams up to the second order. (In the context of perturbation theory, the $\delta$-function approximation of the spectral functions amounts to the lowest order in $g$ Born approximation to the self-energy operator.)

On the other hand, taking the limit $N\to\infty$ gives

$$n_b=\frac{N(e^{\pi g^2/\lambda}-1)}{2e^{\pi g^2/\lambda}+N}. \tag{31}$$

This is the main result of the kinetic equation approach. For $e^{\pi g^2/\lambda}\ll N$ we find

$$n_b=e^{\pi g^2/\lambda}-1. \tag{32}$$

This matches the large-$N$ limit given by Eq. (13).

The kinetic equation produces the boson number (31) which is monotonously increasing with decreasing $\lambda$, until it reaches its limiting small $\lambda$ value of $N/2$. The reason for this behavior is that at large $N$, the r.h.s. of the kinetic equation approaches zero at $n_f=1/2$. In other words, the rate of fermions converting into bosons is matched by the rate of bosons converting into fermions. However, we need to remember that at $n_b=N/2$ we are well outside the regime of validity of the approximated kinetic equation. In fact, we are outside the limit of the RPA as such. This is because at $n_b\simeq N$ diagrams that are nominally small in $N^{-1}$ become sizeable, on account of the large value of the distribution function $n_b\simeq N$. For example, it is straightforward to verify that its crossing interaction lines make the diagram in Fig. 3(b) small in $N^{-1}$, but this smallness gets counteracted by $n_b$-dependent propagators in the center regions of the diagram. The bottom line is that the RPA is controlled only in the limit $n_b/N\to 0$. Our comparison with numerics below will show that it works remarkably well beyond its nominal limits, i.e., profile (31) represents a good approximation even at $n_b/N=O(1)$. However, in order to advance into the adiabatic regime, $n_b\to N$, we need to employ different methods.

## V. SEMICLASSICAL ANALYSIS

Our goal now is to understand the behavior of $n_b$ for arbitrary driving rates $\lambda$. We will use that for large $N\gg 1$ our problem approaches a well-defined classical limit where both spin and the bosonic fields can be treated as classical objects. The classical equations of motion, obtained by replacing operators in the Hamiltonian (4) with $c$ numbers and commutators by Poisson brackets, read

$$i\dot{b}=-\lambda tb+\frac{g}{\sqrt{N}}S^-,$$

$$\dot{S}_z=-i\frac{g}{\sqrt{N}}(bS^+-b^*S^-),$$

$$\dot{S}_x=-i\frac{g}{\sqrt{N}}(b^*-b)S_z-\lambda tS_y,$$

$$\dot{S}_y = -\frac{g}{\sqrt{N}}(b+b^*)S_z + \lambda t S_x. \tag{33}$$

Within the strictly classical setting, these equations have to be solved for the initial conditions $b(t_0)=0$, $S_z(t_0)=N/2$, and $S_x(t_0)=S_y(t_0)=0$, where $t_0\to-\infty$ is the initial time. It is straightforward to verify that the solution corresponding to these initial conditions reads $(b(t),S_z(t))=(b(t_0),S_z(t_0))=(0,N_0)$, i.e., the initial configuration of zero bosons represents a classically stationary (if unstable) solution.

The prediction that no bosons will be generated is clearly wrong. However, the purely classical treatment has yet another, and related, drawback: for given initial conditions the uniqueness of the classical solution does not permit the buildup of fluctuations. This is in contradiction with our earlier findings that the distribution of $n_b$ is wide at least at fast and intermediate rates.

It is thus obvious that a meaningful description of the classical limit must account for the presence of quantum fluctuations. These fluctuations will lead to an initial destabilization of the configuration $(b(t),S_z(t))=(0,N_0)$. The nonlinearity of the classical Hamiltonian then amplifies the fluctuations and drives the system away from its initial state. The expansion of dynamics in quantum fluctuations for bosons was analyzed in detail in Ref. [32]. Using a path integral construction similar to the Keldysh technique it was shown that to leading order in quantum fluctuations the classical (Gross-Pitaevskii) equations of motion do not change. However, the initial conditions become randomly distributed with the weight given by the Wigner transform of the density matrix. This so-called TWA originated in quantum optics [33,34] and has later been adapted to cold atom systems [35]. By now the TWA has become a standard tool in describing the dynamics of cold atoms in regimes where classical Gross-Pitaevskii equations do not suffice (see Ref. [36] for review).

The TWA is most conveniently adapted to our model by using the Schwinger boson representation of spins. The small parameter of this expansion is $1/S$, where $S\to\infty$ describes the classical spin. In Appendix B we give some details of this derivation. The net result is that the classical equations of motion (33) need to be supplied by stochastic initial conditions distributed according to the Wigner function. For large spin (pointing along the $z$ direction) and vacuum state of bosons, representing the initial conditions in our problem, this Wigner function is approximately given by

$$W(n_b,S_z,S_\perp) \approx \frac{2}{\pi S}\exp[-2n_0]\exp\left[-\frac{S_\perp^2}{S}\right]\delta(S_z-S), \tag{34}$$

where $S_\perp=\sqrt{S_x^2+S_y^2}$ and $n_0$ is the initial boson number. The fact that $S_\perp$ and $n_0$ are not exactly equal to zero is the result of vacuum quantum fluctuations. In this work we are primarily interested in the number of bosons created during the dynamical process and its fluctuations. The connection between moments $n_0^l, l=1,2,\ldots$ and the variables $b$ and $b^\dagger$ is established by the Wigner transform identities summarized in Appendix B. For instance,

$$n_0 \to b^*b - 1/2, \quad n_0^2 \to (b^*b)^2 - b^*b. \tag{35}$$

(The correction term $b^*b$ appearing in the expression for the second moment ensures that zero-point fluctuations do not affect the expectation value of $n_0$ and $n_0^2$, which should be zero in the vacuum state. In the classical limit $n_0\gg 1$, these terms become inessential.)

By way of an illustration, let us outline how the TWA reproduces the results of the quantum calculation in the linearizable regime. For quadratic Hamiltonians the TWA is exact [32,33] and we must be able to reproduce all the results of Sec. III. Upon leaving the linear regime, the number of bosons $n(t)=\langle b^\dagger(t)b(t)\rangle$ has become large and semiclassical methods are expected to work with high accuracy. In other words, the exactness of the TWA to the linear regime entails its applicability to the full parameter space of our problem.

In the linear regime, we may assume approximate constancy of $S_z$: $S_z\approx S=N/2$. Equation (33) then reduces to

$$i\dot{b} = -\lambda t b + g s^-,$$

$$i\dot{s}^- = -g b + \lambda t s^-, \tag{36}$$

where we used $s^-=S^-/\sqrt{N}$. These equations are identical to an exact reformulation of the Schrödinger equation [cf. Eq. (A1) in Appendix A], a consequence of the linearity of the problem. In Appendix B, Sec. B 3 we show that the solution of these equations, with account for quantum fluctuations in the initial data, indeed reproduces the results of the full quantum calculation. In particular we show there that $n_b=x-1$ and $\langle n_b^2\rangle=2x^2-3x+1$ [here as before, we reserve the notation $n_b$ for the number of bosons at the end of the process, as in Eq. (5)]. Both results perfectly agree with the exact distribution (14).

At slow values of driving, $x\sim N$ the nonlinear equations (33) no longer afford an exact solution. In Sec. VI we will discuss an approximate solution scheme, based on the method of adiabatic invariants. In Sec. VII we will analyze in detail $n_b(\lambda)$ and its distribution in various regimes using both exact and TWA simulations.

## VI. DEEP ADIABATIC LIMIT

### A. Adiabatic Hamiltonian

In this section, we will apply the concept of classical adiabatic invariance to the adiabatic limit of the driving process. Considering a fixed initial value $n_0\sim 1$ [consistent with Eq. (34)], we will be sloppy about initial conditions. This is good enough to obtain reliable results for the mean value of produced bosons, $\langle n_b\rangle$, but will not suffice to obtain the statistics of the driving process. The latter will be explored in Sec. VII below within the more sophisticated TWA scheme.

The concept of the adiabatic evolution of classical invariants [37] was previously applied to the semiclassical limit of a nonlinear Schrödinger equation [10] and later [13] to the classical equations of our model. However (for all but very small, compared with $N$, initial occupancy $n_0\sim 1$) the latter reference predicts a power law $\sim\lambda^{1/3}$ for the conversion rate which we can exclude on the basis of direct numerics, TWA,

and our analytical calculation below. Yet, the conceptual basis for the emergence of power laws (as opposed to exponentials such as in the original Landau-Zener problem) remains valid: in driven classical dynamical systems, certain invariants of the autonomous limit of the evolution (viz. the action picked up upon traversal of periodic trajectories) become weakly time dependent. While in most regions of phase space this time dependence is very (exponentially in the driving rate) weak, it can become strong (algebraic) in the vicinity of singular points. Such points reflect the presence of nonlinearities in the Hamiltonian, which in our problem are due to interactions. When the driving parameter sweeps across a singular point, the topology of trajectories in phase space (and thence the action picked up along these trajectories) may change profoundly. It is the dynamics of these processes which we will investigate in the following. Specifically, we will consider the system in the following limit:

$$N \gg 1, \quad \frac{\lambda}{g^2} \ll 1, \quad \frac{1}{N^\alpha} \ll \frac{\lambda}{g^2} \ln N \ll 1, \tag{37}$$

where $\alpha > 0$ is an arbitrary positive number.

We consider the Hamiltonian (4) in the limit of $c$-number-valued operators. Using a number-phase decomposition of the boson field, $b \to \sqrt{n} e^{i\varphi}$, and a polar representation of spin variables, $S_z = S\cos\theta$, $S_x = S\sin\theta\cos\xi$, and $S_y = S\sin\theta\sin\xi$, it assumes the form

$$H(n,\varphi,\theta,\xi) = -\lambda t n + \lambda t \frac{N}{2}\cos\theta + g\sqrt{Nn}\sin(\theta)\cos(\xi-\varphi).$$

The two angles $\xi$ and $\varphi$ can be combined into one angle $\phi = \xi - \varphi + \pi$ (where $\pi$ is added for later convenience). The angle $\theta$ and the boson number $n$ are not independent, but are related via the conservation law

$$n = \frac{N}{2}(1-\cos\theta). \tag{38}$$

This allows us to trade $\theta$ for $n$. It is then convenient to rescale

$$n \to Nn, \tag{39}$$

so that the new $n$ varies from 0 to 1, with the last value taken when all particles are bosons. Similarly, the rescaled initial condition reads

$$n_0 \sim \frac{1}{N}.$$

It is also advantageous to replace

$$H \to NH. \tag{40}$$

Throughout this section, we will work with the rescaled variables as described here, restoring the original variables at the end.

Finally, without any loss of generality we can set $g=1$ since it can be scaled out by the appropriate rescaling of $t$. We arrive at the Hamiltonian

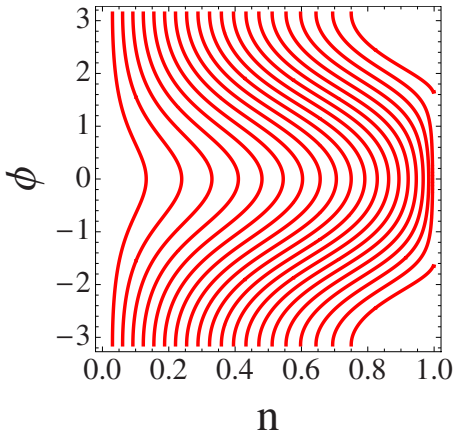


FIG. 4. (Color online) Trajectories of $H$ at $\gamma=-3$. Here the horizontal axis is $n$, varied from 0 to 1, and the vertical axis is $\phi$, varied from $-\pi$ to $\pi$.

$$H = -\gamma n - 2n\sqrt{1-n}\cos(\phi), \quad \gamma = 2\lambda t. \tag{41}$$

Here $\phi$ and $n$ play the role of the coordinate and momentum, canonically conjugate to each other. The equations of motion of these variables read as

$$d_t n = -\partial_\phi H,$$

$$d_t \phi = \partial_n H. \tag{42}$$

These equations of motion need to be supplied with initial conditions. In this section, where the emphasis is on the calculation of the "typical" number of produced bosons, we will supply the dynamical system (42) with a fixed value of the initial $n$. We take this to be the typical value $n_0 \sim 1/N$ of the (rescaled) distribution (34). [As we will see below in the slow limit $n(t\to\infty)$ has only logarithmic sensitivity to $n_0$ and precise form of the initial value is not important, as long as we are interested in estimating mean conversion rates. For the same reason the initial fluctuations in the angle $\theta$, which we ignored, are also unimportant.]

We begin our analysis of the initial value problem by plotting lines of constant energy $H=$const at different fixed values of $\gamma$. Examples are shown in Figs. 4–7. The lines shown in these figures represent trajectories of the Hamiltonian for $\gamma$ fixed. In our problem, $\gamma$ changes in time. However, at small $\lambda$, $\gamma$ changes slowly. Thus the system will follow one of the trajectories for some time before it will slowly drift to a different trajectory due to the slowly changing $\gamma$.

### B. Fixed points

An important role in our analysis is played by the fixed points of the Hamiltonian system [10,11,13]. This is where the trajectory consists of a single point ($\gamma$ still kept fixed). They are found by solving

$$\frac{\partial H}{\partial \phi} = 0, \quad \frac{\partial H}{\partial n} = 0. \tag{43}$$

There are two families of solutions $(n,\phi)$ of these equations (in addition to the trivial solution $n=0$ appearing for $\gamma >$

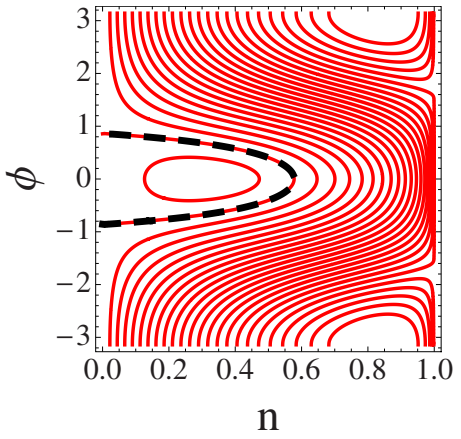


FIG. 5. (Color online) Trajectories of $H$ at $\gamma=-1.3$. The critical trajectory is shown as a dashed (black) line.

$-2$). The first exists for $-2<\gamma<2$ and has $\phi=0$, $(n,\phi)\equiv(n_1(\gamma),0)$, where

$$n_1(\gamma)=\frac{12-\gamma^2+\gamma\sqrt{12+\gamma^2}}{18}. \tag{44}$$

This solution appears at $n_1(2)=0$ at $\gamma=-2$. As $\gamma$ is increased above $-2$, $n_1(\gamma)$ starts increasing until it asymptotically reaches $\lim_{\gamma\to\infty} n_1(\gamma)=1$.

The other solution has $\phi=\pi$ and requires $\gamma<2$. It is given by

$$n_2(\gamma)=\frac{12-\gamma^2-\gamma\sqrt{12+\gamma^2}}{18}. \tag{45}$$

This solution appears at $n_2(2)=0$. As $\gamma$ is decreased below 2, $n_2(\gamma)$ starts increasing and asymptotes as $\lim_{\gamma\to-\infty} n_2(\gamma)=1$.

We thus arrive at the following picture. Initially the number of bosons is given by $n=n_0\sim 1/N$ at undetermined $\phi$. The coordinates $n$ and $\phi$ evolve according to the approximate Hamiltonian $H\approx-\gamma n$, where we used that at large negative times $\gamma$ is very large to keep only the leading-order contribution in this scale. This means that the motion is initially given by

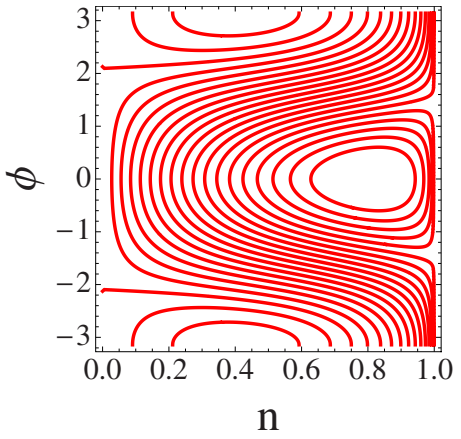


FIG. 6. (Color online) Trajectories of $H$ at $\gamma=1$.

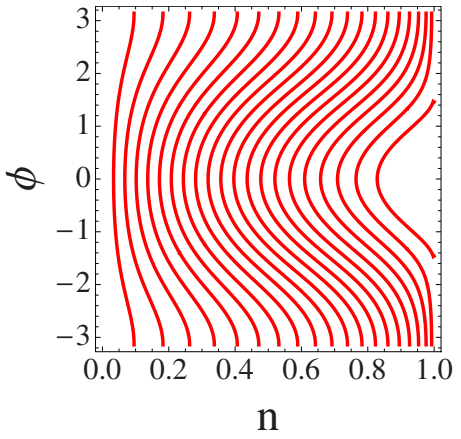


FIG. 7. (Color online) Trajectories of $H$ at $\gamma=4$. The U-shaped trajectory on the right of the picture is *not* critical, despite looking superficially similar to the critical trajectory shown on Fig. 5.

$$n=\frac{1}{N},\quad \phi=-\gamma t. \tag{46}$$

However, as $\gamma$ is increasing, the fixed point $n_1(\gamma)$, given by Eq. (44), appears at the critical value $\gamma=-2$. As $\gamma$ keeps increasing the point moves toward larger values of $n$. At a certain moment of time, the trajectory $(n,\phi)(t)$ will drastically change: it will no longer perform extended propagation in $\phi$ directions but start winding around the fixed point (45). Eventually, at some large positive $\gamma$, the trajectory will stop winding around the fixed point and merge into a new extended trajectory, which at large positive $\gamma$ will take the form

$$n=n_b,\quad \phi=-\gamma t. \tag{47}$$

$n_b$ is the final number of bosons we are trying to calculate.

The fixed point $n_1(\gamma)$ has an intimate relationship with the instantaneous ground state of the quantum Hamiltonian (4). This is discussed in more details in Appendix C.

### C. Adiabatic invariants

In the classical mechanics of slow parameter-dependent Hamiltonians there exist approximately conserved "adiabatic invariants" [37]. Generally, adiabatic invariants assume the form of action integrals $\sim\int pdq$, where the integral is over one full revolution of the system's motion. In the present context, the invariant is given by

$$I=\frac{1}{2\pi}\int d\phi n. \tag{48}$$

To further elucidate the meaning of the adiabatic invariant in our problem, let us go back to the angular variable $\theta$ according to Eqs. (38) and (39). We find

$$I=\frac{1}{4\pi}\int d\phi(1-\cos\theta). \tag{49}$$

This is nothing but the area of a part of the surface of a unit radius sphere bounded by the trajectory $\theta(\phi)$, where $\theta$ and $\phi$ are thought of as spherical angles divided by $4\pi$. This geo-

metric definition of the adiabatic invariant implies an ambiguity which needs to be resolved. A closed trajectory on the surface of a unit sphere separates the surface into two domains, and one needs to pick the area of one of them.

We define the adiabatic invariant as the area (divided by $4\pi$) of the domain on the surface of the unit sphere bounded by the trajectory such that the trajectory, when the domain is viewed from above, encircles the domain in the counterclockwise direction. We note that this definition does not always conform to the algebraic expression (48). However, it results in the adiabatic invariant continuous under smooth deformations of the trajectory, while Eq. (48) can be discontinuous under those transformations.

For trajectories such as the initial trajectory (46) or the final trajectory (47) the adiabatic invariant is very easy to calculate. Initially the trajectory encloses the north pole of the sphere in the counterclockwise direction to result in

$$I_{\text{initial}} \equiv I(\gamma \to -\infty) = \frac{1}{2\pi}\int_{-\pi}^{\pi} d\phi\, n(\gamma \to -\infty) \sim \frac{1}{N}.$$

At the end of the process Eq. (47) implies that the trajectory now encloses the south pole in the counterclockwise direction. The adiabatic invariant is now given by

$$I_{\text{final}} \equiv I(\gamma \to \infty) = 1 - \frac{1}{2\pi}\int_{-\pi}^{\pi} d\phi\, n(\gamma \to \infty) = 1 - n_b. \tag{50}$$

In the limit $\lambda \to 0$, $I$ is conserved;

$$I_{\text{final}} = 1 - n_b \sim \frac{1}{N}. \tag{51}$$

This implies that at the end oft the process all particles become bosons, $n_b \approx 1$ (with $1/N$ factor coming from a quantum uncertainty irrelevant in the large-$N$ limit).

As the rate $\lambda$ is increased, the adiabatic invariant starts changing with time. In Sec. VI D, we will review the general theory of adiabatic action changes and then apply it to our particular problem at hand. Readers not interested in details of the adiabatic dynamical evolution of the system may just note the final result of our analysis, Eq. (63).

### D. Theory of approximate conservation of the adiabatic invariants

The theory of approximate conservation of adiabatic invariants is a well-developed subject, described in detail in Ref. [37]. One of its main results is that the change in an adiabatic invariant during some time-dependent process is usually exponentially suppressed at slow rate,

$$\Delta I \sim \exp\left(-\frac{\text{const}}{\lambda}\right), \tag{52}$$

where $\lambda$ is the rate of the process. In fact, one may interpret the standard Landau-Zener transition probability in terms of this behavior.

However, the theory also states that if a singularity develops at a certain time during the evolution, Eq. (52) breaks down and gets replaced, typically, by a power law. We are going to see that this is indeed the case in our problem.

For the convenience of the reader, we briefly summarize the essentials of the theory of adiabatic invariants, as discussed in Chaps. 49 and 50 of Ref. [37]. Consider a Hamiltonian $H=H(\phi,n,\gamma)$ depending on a pair of conjugate variables $(\phi,n)$ and a slowly varying parameter $\gamma$. For starters, assume $\gamma$ to be constant. Since $H$ describes a system with only one degree of freedom, we have integrability and it is convenient to transform to canonical or "action-angle" variables. The action variable is defined as

$$I = \frac{1}{2\pi}\oint d\phi\, n(E,\phi,\gamma),$$

where the integral is over a closed trajectory of the system's evolution. Such curves are specified by a value of the conserved energy $E$ and, in our case, by the value of $\gamma$. We thus have a functional relation $I=I(E,\gamma)$. Now, consider the so-called abbreviated action

$$S(\phi,E,\gamma) \equiv \int_{\phi_0}^{\phi} d\phi'\, n(E,\phi',\gamma),$$

where the integral extends only over a certain segment of the trajectory. The relation $I=I(E,\gamma)$ may be inverted to express $S$ as

$$S(\phi,E(I,\gamma),\gamma) = S(\phi,I,\gamma)$$

as a function of the coordinate and the action variable. The abbreviated action is the generator of a canonical transformation $(\phi,n)\to(I,w)$ from the old coordinates to the (conserved) action and a conjugate angular variable. Specifically, we have the relation $n=\partial_\phi S(\phi,I,\gamma)|_I$ and define the angular variable as $w \equiv \partial_I S(\phi,I,\gamma)|_\phi$. The equations of motion in the new variables read

$$d_t I = -\frac{\partial H'}{\partial w},$$

$$d_t w = \frac{\partial H'}{\partial I},$$

where $H'=H'(I,w,\gamma)$ is the Hamiltonian expressed in terms of new variables. For an autonomous system ($\gamma$=const), $H'(I,w,\gamma)=H(I,\gamma)\equiv E(I,\gamma)$ is but the old Hamiltonian expressed in terms of the action variable. In this case, the action is conserved and the angle varies as $w=t\partial_I E$. During each period of the motion, the action changes by an amount $\Delta S=2\pi I$. The relation $w=\partial_I S$ then implies a change in $w$ by $2\pi$. Thus,

$$w(t) = t\frac{2\pi}{T}.$$

For a nonautonomous system, classical mechanics states that

$$H'(I,w,\gamma) = H(I,\gamma) + \frac{\partial S}{\partial t} = H(I,\gamma) + \frac{\partial S}{\partial \gamma} d_t \gamma,$$

where $S$ on the r.h.s. must be expressed as a function of $(I,w)$ after the parameter differentiation. In other words,

$$H'(I,w,\gamma) = H(I,\gamma) + \Lambda(I,w,\gamma)d_t\gamma,$$

where

$$\Lambda(I,w,\gamma) = \left.\frac{\partial S(I,\phi,\gamma)}{\partial\gamma}\right|_{\phi=\phi(I,w,\gamma)}. \tag{53}$$

This then means that the action changes and it does so according to

$$d_t I = -\frac{\partial\Lambda(I,w,\gamma)}{\partial w}d_t\gamma. \tag{54}$$

The change in the action over a finite interval of time then follows as

$$\Delta I = -\int dt\frac{\partial\Lambda(I,w,\gamma)}{\partial w}d_t\gamma = -2\lambda\int\frac{dw}{\omega}\frac{\partial\Lambda(I,w,\gamma)}{\partial w}, \tag{55}$$

where

$$\omega \equiv \frac{2\pi}{T}$$

is the characteristic frequency of the trajectory. For time-independent $\gamma$, the integral is over one full interval of a $w$-periodic integrand and vanishes; it is temporal variations in $\gamma$ that give it its finite value. The relations above express the evolution of the action entirely in terms of quantities that do not contain explicit time dependence. One may argue that $\Delta I$ evaluate to Eq. (52), unless the time dependence of $\omega^{-1}$ and $\partial\Lambda$ contains singularities. This will turn out to be the case in our problem.

Figures 4–7 show examples of trajectories that enter the computation of action integrals for our dynamical system. (Each of these trajectories corresponds to a particular value of $I$ while $w$ parametrizes the trajectory.) In computing the above integrals, we will then be met with the following scenario: consider a trajectory close to the left boundary of phase space and at an initial value $\gamma \ll 0$. Initially, that trajectory will be "open," i.e., its angular variable will periodically run from 0 to $2\pi$, at moderately changing $n$. To the trajectory we may assign an instantaneous value of energy $H(n,\phi,\gamma)$, which changes on account of increasing $\gamma$. As $\gamma$ approaches the value $-2$ from below, we run into a singularity: at a certain value $\gamma=-2+\epsilon_0$, where $0<\epsilon_0\ll 1$, the energy vanishes, $H(n,\phi,-2+\epsilon_0)=0$. That point marks a drastic change in the topology of the trajectory; it changes from open to closed. See Fig. 5 for an example of a closed trajectory and a "critical" trajectory with $H=0$. The latter begins and ends at $n=0$ and has the form of a horizontally aligned horseshoe. The passage time through the critical trajectory is infinite, and it is logarithmically divergent on the closed trajectories for $\epsilon \searrow \epsilon_0$ (in contrast, it can be checked that another U-shaped trajectory, which starts and ends at $n=1$ and can be seen on Fig. 7, is not critical and its passage takes finite amount of time). The action integral receives its dominant contribution from a range of $\epsilon$ values above $\epsilon_0$.

To describe this situation algebraically, we expand the Hamiltonian (41) for small $\epsilon$, $n$, and $\phi$, where

$$\gamma = -2+\epsilon$$

as

$$H = n(\phi^2 - \epsilon + n).$$

The singular trajectory is given by $H=0$ or $n=\epsilon-\phi^2$. Its frequency is zero (the period is infinity) and its adiabatic invariant is given by

$$I = \frac{1}{2\pi}\int_{-\sqrt{\epsilon}}^{\sqrt{\epsilon}} d\phi(\epsilon-\phi^2) = \frac{2}{3\pi}\epsilon^{3/2}. \tag{56}$$

The trajectories inside the singular trajectory have $H<0$ (one of these is shown in Fig. 5). On these closed trajectories, $n$ is a two-valued function of $\phi$, where the two branches $n_\pm(\phi)=\frac{1}{2}\{\epsilon-\phi^2\pm[(\phi^2-\epsilon)^2+4H]^{1/2}\}$ represent the right and left bending arcs as $\phi$ varies in $-\sqrt{\epsilon-2\sqrt{-H}}\le\phi\le\sqrt{\epsilon-2\sqrt{-H}}$. The action of these curves equals the area enclosed by the trajectories, divided by $2\pi$, or

$$I = \frac{1}{2\pi}\int_{-\sqrt{\epsilon-2\sqrt{-H}}}^{\sqrt{\epsilon-2\sqrt{-H}}} d\phi\sqrt{(\phi^2-\epsilon)^2+4H}$$
$$\approx \frac{\epsilon^{3/2}}{2\pi}\left\{\frac{4}{3}-\frac{H}{\epsilon^2}\left[\ln\left(-\frac{H}{16\epsilon^2}\right)-1\right]\right\}. \tag{57}$$

This expression is approximate and valid for small $|H|\ll\epsilon^2$. The corresponding frequencies are given by

$$\omega = \frac{\partial H}{\partial I} = -\frac{2\pi\sqrt{\epsilon}}{\ln\left(-\frac{H}{16\epsilon^2}\right)}. \tag{58}$$

These frequencies indeed vanish logarithmically as $H\nearrow 0$ approaches zero, confirming that the $H=0$ trajectory is critical.

The mechanical system we need to study starts its evolution at $t\to-\infty$ by moving according to Eq. (46). Subsequently, at a time where $\gamma$ is slightly larger than $-2$, the system crosses the singular trajectory and starts moving around the fixed point (45). It is at this time that the adiabatic invariant receives most of its increase.

We estimate the increase by first calculating $S$ for the part of the trajectory represented by $n_-(\phi)$, where $\phi<0$

$$S = \frac{1}{2}\int_0^\phi d\phi'[\epsilon-\phi'^2-\sqrt{(\phi'^2-\epsilon)^2+4H}].$$

In this formula, $H=H(I)$ must be understood as a function of $I$, which can be found by inversion of Eq. (57). We then calculate $\Lambda$ according to Eq. (53) as follows:

$$\Lambda = \frac{1}{2}\int_0^\phi d\phi'\left[1-\frac{\epsilon-\phi'^2+2\frac{\partial H}{\partial\epsilon}}{\sqrt{(\epsilon-\phi'^2)^2+4H}}\right],$$

where $\phi$ has to be substituted by $\phi=\phi(I,w,\phi)$ after the integration. We now use this result to compute the time variation of the action according to Eq. (54). Using that the $w$ dependence of $\Lambda$ is in $\phi(w,I,\lambda)$ and that $d_t\gamma=2\lambda$, we have

$$d_t I = -2\lambda \frac{\partial \Lambda}{\partial \phi}\frac{\partial \phi}{\partial w} = -\lambda\left[1 - \frac{\epsilon - \phi^2 + 2\frac{\partial H}{\partial \epsilon}}{\sqrt{(\epsilon-\phi^2)^2+4H}}\right]\frac{\partial \phi}{\partial w}.$$

Eventually, this quantity has to be integrated over time, and to do so we need information on the time dependence of $\phi(I,w,\gamma)=\phi(I,\omega t,\gamma)$. The equations of motion tell us

$$d_t \phi = \partial_n H = -\sqrt{(\epsilon-\phi^2)^2+4H}. \tag{59}$$

We next assume that during the time when the invariant $I$ receives most of its increase, $\phi$ takes values such that the r.h.s. of this equation vanishes. The validity of this presumption will be checked in the end of the section. This implies

$$\phi \sim -\sqrt{\epsilon}. \tag{60}$$

Indeed, everything done so far implies $|H| \ll \epsilon^2$ and so the right-hand side of Eq. (59) approximately vanishes if Eq. (60) holds.

Using this stationarity condition and $\partial_w \phi = \omega^{-1} d_t \phi$ we obtain

$$d_t I \simeq \frac{2\lambda}{\omega}(\sqrt{-H} - \partial_\epsilon H).$$

In this equation $H=H(I,\epsilon)\ll\epsilon^2$ is implicitly defined by Eq. (57). This gives

$$\frac{\partial H}{\partial \epsilon} = -\frac{\partial I}{\partial \epsilon}\left(\frac{\partial I}{\partial H}\right)^{-1} \simeq \frac{2\epsilon}{\ln\left(-\frac{H}{16\epsilon^2}\right)},$$

a term that is larger than the $\sqrt{-H}$ contribution to $d_t I$. Using Eq. (58), we arrive at the estimate

$$d_t I \simeq \frac{2\lambda \epsilon^{1/2}}{\pi}.$$

Using $\epsilon = 2+2\lambda t$, we integrate this expression over $\epsilon$ from $\epsilon=\epsilon_0$, remembering that $I=2\epsilon_0^{3/2}/(3\pi)$ when $\epsilon=\epsilon_0$, to find

$$I \simeq \frac{2}{3\pi}\epsilon^{3/2}. \tag{61}$$

This expression looks formally identical to Eq. (56), but has a different meaning. While Eq. (56) is the adiabatic invariant of the critical trajectory, Eq. (61) signifies that this expression remains approximately true even at later times when the system no longer follows the critical trajectory.

We finally need to find the maximum value $\epsilon \equiv \epsilon^*$ for which Eq. (61) still holds (at even higher values of $\epsilon$, the adiabatic invariant will stop growing and just oscillate about its average value). The criterion we will use to determine that value reads $w=\pi$, i.e., we demand that the system proceeded along half a period of the critical trajectory. At larger instances of time ($\epsilon$) the transit into the domain of oscillatory motion and no further systematic action increase has taken place. In practice, the fixation of $\epsilon^*$ turns out to be somewhat tedious, and we have relegated it into Appendix D. As a result we obtain

$$\epsilon^* \sim \left(\frac{3}{2}\lambda \ln N\right)^{2/3}. \tag{62}$$

Finally, with the help of Eq. (51) this leads to our final answer

$$n_b \simeq N\left(1 - \frac{\lambda}{\pi g^2}\ln N\right), \tag{63}$$

where we have reconsidered the coupling strength $g$ and returned to the original (unrescaled) $n_b$. Note that in the derivation above we relied only on the fact that the unrescaled $n_0 \sim 1$ due to quantum fluctuations. If we start from the state where $n_0$ is nonzero (but smaller than $N$) due to initial occupancy of the molecular state, result (63) remains valid with the only difference that the argument of the logarithm should be changed to $N/n_0$. This is qualitatively different from the results of Ref. [13] where an instant crossover to a $\sim\lambda^{1/3}$ power law the moment $n_0 \gtrsim 1/N$ was predicted. In our analysis we do not find such a regime either analytically or numerically for any $n_0$.

## VII. TWA AND COMPARISON WITH NUMERICAL SIMULATIONS

In this section, we will apply a combination of numerical diagonalization and the TWA to obtain accurate results for both the mean value of $n_b$ and its distribution. For moderate values of $N$, the Schrödinger equations for Eq. (4) can be solved directly. Indeed, the Hilbert space corresponding to that Hamiltonian, in the sector $S_z + b^\dagger b = N/2$, has only $N+1$ states. Thus the Hamiltonian reduces to a $(N+1)$-dimensional matrix. This matrix can be diagonalized at reasonable numerical cost up to values $N \lesssim 10^3$ (see Appendix C for an example of how this procedure can be set up).

At larger values of $N$, we simulate the classical equations of motion, with initial conditions drawn from the quantum Wigner distribution (34)—the TWA. In this way, we may obtain results for significantly larger values of $N$. In the following we will apply both methods interchangeably. However, before doing so, let us first test the accuracy of TWA by comparison to numerical diagonalization at values of $N$ where both methods are applicable.

### A. TWA versus direct diagonalization

In Sec. V we have argued that the exactness of the TWA in the linear regime entails its applicability to the whole range of driving parameters. To back up this claim, let us compare TWA results to those obtained by numerical diagonalization. In Fig. 8 we show $\langle n_b\rangle(\lambda)$ for two values of $N=2S$: $N=64$ and $N=128$. The solid and dashed lines represent the exact and TWA solutions, respectively. There is no visible difference between them. To demonstrate that TWA is not actually exact we show in the inset the difference between TWA and numerical results multiplied by a factor of 100. Clearly for $N=128$ the accuracy of TWA is better which signals that as $N$ increases TWA gives results of increasing precision.

In Fig. 9 we plot the relative number fluctuations $\delta n_b/N = \sqrt{\langle n_b^2\rangle - \langle n_b\rangle^2}/N$ as a function of $\lambda$ for $N=64$. As with the dependence $n_b(\lambda)$ the difference between TWA and exact results is minuscule and it vanishes fast as $N$ gets larger.

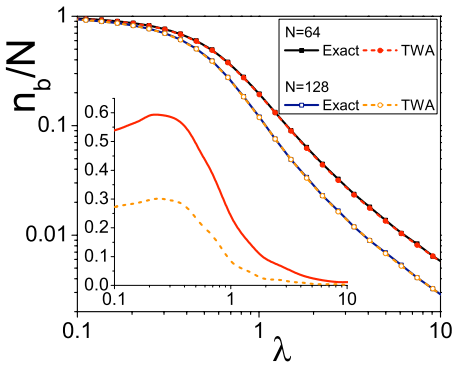


FIG. 8. (Color online) Dependence of the scaled number of bosons $n_b/N$ as a function of the rate λ. The two pairs of curves correspond to $N \equiv 2S = 64$ and $N = 128$. The solid lines represent the exact solution while the dashed lines are the semiclassical TWA. The inset shows the difference between exact and semiclassical results ($N = 64$ red solid line and $N = 128$ orange dashed line) multiplied by a factor of 100.

These results make us confident that TWA represents high-precision method which becomes asymptotically exact in the limit $N \to \infty$.

### B. Combined application of TWA and direct diagonalization

In the following we will analyze our system by combined application of the two numerical methods. We will not indicate which method was used for which particular curve, unless necessary. In all numerical simulations we set $g = 1$. (This can be always achieved by the rescaling $\lambda \to \lambda g^2$.) Unless stated differently, the notation $n_b(\lambda)$ refers to the mean value of the number of bosons.

In Fig. 10 we plot $n_b(\lambda)$ for different values of $N$. For small $N$ the function $n_b(\lambda)$ is qualitatively similar to an exponential form $n_b(\lambda)/N \propto 1 - 1/x = 1 - \exp(-\pi/\lambda)$, as with the conventional two-level Landau-Zener problem. However, as $N$ increases this exponential behavior disappears and the dependence becomes much closer to the linear one predicted in Eq. (63). To demonstrate the approach to linear scaling, we plot $n_b(\lambda)$ for large values of $N$ up to $N \sim 10^8$ in Fig. 11. The

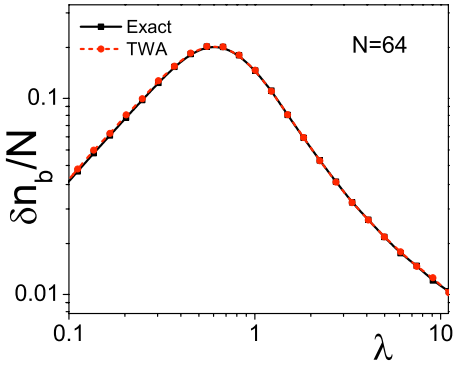


FIG. 9. (Color online) Dependence of the scaled standard deviation of the number of bosons $\delta n_b/N$ after the process as a function of the rate λ for $N = 64$. The two curves represent the exact and the TWA results.

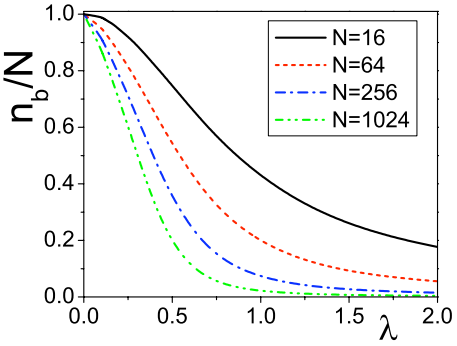


FIG. 10. (Color online) Number of remaining bosons $n_b$ vs the rate λ for different values of $N$. It is clear that as $N$ increases the dependence goes from exponential form characteristic for Landau-Zener process to the linear one predicted analytically [see Eq. (63)].

dashed line is the fit to the linear dependence $n_b/N \approx 1 - 0.28\lambda \ln N$. Note that the prefactor 0.28 is slightly different from the $1/\pi$ in Eq. (63). But given that the analytical result was obtained using a series of approximations we find this level of agreement to be satisfying.

Figure 12 shows the results of numerical simulations at $N = 10^3$, $N = 10^4$, $N = 10^6$, and $N = 10^8$ plotted as $(1 - n_b/N)/\ln N$ vs $\lambda/(\pi g^2)$. The straight line in the plot represents the deep adiabatic limit Eq. (63), while the second continuous line is the solution of the kinetic equation (31) at $N = 10^3$ only.

We see that the deep adiabatic relation (63) is confirmed in the limit of slow rates. As to the solution of the kinetic equation, while it describes well the relatively fast rates, it deviates from the numerics at slower rates and eventually breaks down when it saturates at nonzero value when $\lambda \to 0$.

Next, let us discuss the distribution function $P(n_b)$. In the fast limit we have a well-defined analytical prediction given by Eq. (14). It matches the numerical simulations very well, as shown in Fig. 13. While for the slow limit we do not have an analytical prediction for the distribution function, one can make a good ansatz based on result (63). Note that this result was obtained for a particular choice of $n_0 = 1$. More generally for each fixed initial value of $n_0$ it should read

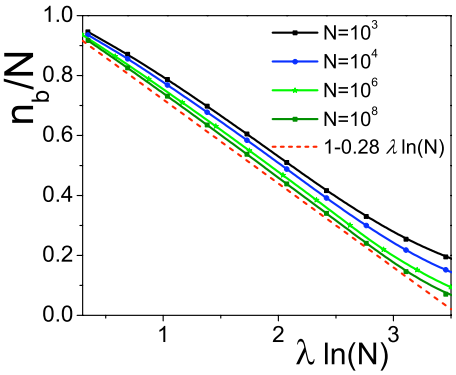


FIG. 11. (Color online) Same as in Fig. 10 but for large values of $N$. Note that the horizontal axis is $\lambda \ln N$.

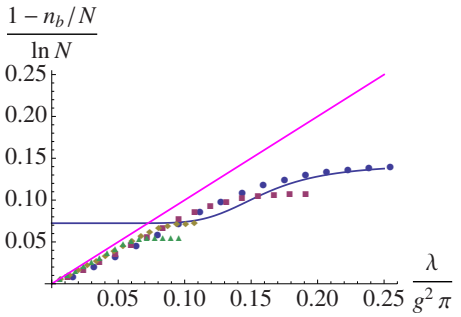


FIG. 12. (Color online) Number of remaining bosons $n_b$ vs the rate λ for different values of $N$. Here circles represent $N=10^3$, squares $N=10^4$, rhombi $N=10^6$, and triangles $N=10^8$. The continuous lines represent our analytical solutions, as discussed in the text.

$$n_b(n_0)/N \approx 1 - \frac{\lambda}{C_1}\ln(C_2 N/n_0), \tag{64}$$

where $C_1$ is a constant close to $\pi$ and $C_2$ is another constant, which in general can depend on λ. Finding this constant is beyond accuracy of our analytical derivation. Because we know the distribution of $n_0$: $P(n_0)=2\exp[-2n_0]$ we can invert Eq. (64) and derive the distribution function of $n_b$ as follows:

$$P(n_b) \approx 2\frac{C_1}{\lambda}C_2 e^{-\rho}\exp[-2C_2 N e^{-\rho}],$$

$$\rho = \frac{C_1}{\lambda}\left(1-\frac{n_b}{N}\right). \tag{65}$$

The function $P(n_b)$ above describes the Gumbel distribution, which often appears in the context of the extreme value statistics.

It is interesting to note that according to the theorem proven in Ref. [50], $P(0)=\exp(-\pi g^2\lambda)$. It is straightforward to see that Eq. (66) and Eq. (14) are indeed consistent with this result within their respective applicability ranges.

We plot the distribution function $P(n_b)$ in Fig. 14. The solid lines are the result of the TWA approximation and the dashed lines are the exact result. At slow rates the distribution function becomes highly asymmetric. At $\lambda=0.2$ it is very well fitted by the Gumbel distribution (65) (gray dotted line) with $C_1\approx 3.05$ (instead of $\pi$) and $C_2\approx 0.03$. The fact that $C_2$ is so small probably indicates that this constant depends on λ. We checked that the fit also works well for $N=256$ with the same constants $C_1$ and $C_2$. From Fig. 14 it is apparent that the semiclassical approximation correctly predicts the Gumbel-type shape of the distribution function at small λ but misses the oscillations on top of this shape. These oscillations have a minor effect on the expectation value of $n_b$ and on its fluctuations. However, they are not negligible and they do not vanish if we increase $N$ (at least they persist up to $N=512$). We are not sure what the origin of these oscillations is. It is interesting to point out that a similar interpolation of the distribution function from the exponential to the Gumbel form was found in the completely different context of interference between two independent Luttinger liquids [38].

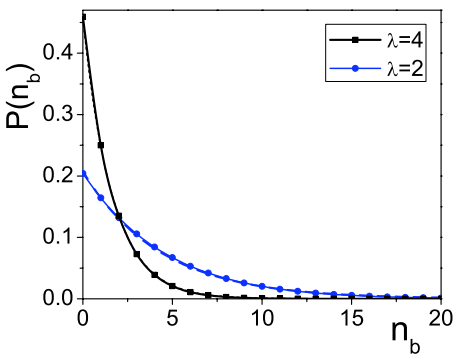


FIG. 13. (Color online) Distribution function of $n_b$ for $N=128$ and two values of the rate: $\lambda=2$ and $\lambda=4$. The distributions are discrete and the lines are the guide for the eyes. The dashed lines, which are barely distinguishable from the numerically computed solid lines, are the analytical prediction (14).

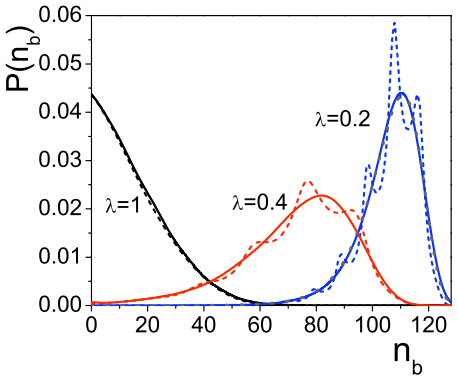


FIG. 14. (Color online) Distribution function of $n_b$ for $N=128$ at $\lambda=1$, 0.4, 0.2. The solid lines are the result of the semiclassical TWA approximation and the dashed lines are the distributions obtained by exact diagonalization. The dotted gray line (which almost coincides with the solid blue line) is the fit to the Gumbel distribution (65) with $C_1\approx 3.05$ and $C_2\approx 0.03$.

### C. Discussion

Result (63) implies that the thermodynamic limit of our system never behaves adiabatically: no matter how small the driving, in the limit $N\to\infty$, the adiabatic limit becomes elusive. Such type of behavior has been found earlier [39] for more general low-dimensional bosonic systems near instabilities such as second-order phase transitions. The giant quantum fluctuations accompanying this nonadiabatic behavior result from the inversion of the classical ground states of the participating systems. Zero-point fluctuations are required to trigger a macroscopic inversion of state occupancies and the stochastic nature of this initiation process generates vast fluctuations at later stages.

Finally, it is worthwhile putting the results above in a more general context: a number of previous works [40–46] have addressed the slow dynamics of low-dimensional critical systems. In all these cases it has been argued that the

number of excitations produced upon slow driving scales as a power law of the rate (as opposed to the exponential dependence Eq. (2) for the Landau-Zener problem.) The exponent of this power law is related to the critical exponents characterizing the phase transition [40,41] under consideration. In low dimensions with their relatively higher density of low-energy states there is a stronger tendency for smaller powers, i.e., less adiabatic regimes. In a sense, our "infinite-range interaction" or "mean-field" system exemplifies these structures in the extreme setting of a zero-dimensional system.

## VIII. APPLICATION TO OTHER DRIVING PROCESSES

We spent most of this paper discussing driving processes where the bosonic sector of the system was initially empty [or there were no atoms in the language of the atom-molecular conversion systems (8) and (10)]. For these initial conditions, quantum fluctuations are needed to jump start boson (or molecule) production, and this is what ultimately leads to the power law (63). We here briefly discuss the "inverse" problem, where initially all $N$ particles were bosons (or atoms). This variant was previously discussed in Ref. [29]. What makes it different, is that no quantum fluctuation is required to start the conversion process. Solution of the classical equations of motion (41) at inverted driving rate, $\gamma=-2\lambda t$, and with initial condition $n(t\to-\infty)=N$ captures the dynamics of the process and quantum fluctuation introduce only minor corrections.

As a result of a straightforward adaptation of the discussion of Sec. IV, we find that the number of bosons $n_b$ for Eq. (4) in the infinite future behaves as

$$n_b \simeq \frac{N}{2-e^{-\pi g^2/\lambda}}. \tag{66}$$

At fast rates, this is equivalent to $n_b \simeq N e^{-\pi g^2/\lambda}$, $\lambda \gg \pi g^2$, which is but the standard Landau-Zener prediction. As the rate slows down, below $x=e^{\pi g^2/\lambda}\sim 1$ the Landau-Zener prediction breaks down. [Notice that the initial (linear) regime in the direct problem was much more robust.]

Taken at a face value, Eq. (66) predicts that at slow driving rates $n_b$ saturates at 1/2. This cannot be correct since Eq. (66) must break down at slower rates. A detailed analysis involving the quasiclassical Hamiltonian (41) with the initial condition $n_0=1$ gives

$$n_b/N \simeq 0.057\lambda, \tag{67}$$

where the constant of proportionality 0.057 was determined numerically from the linear fit [note that unlike that in Eq. (63), it is $N$ independent]. In Fig. 15 we show numerical data for the dependence $n_b(\lambda)$ for the inverse problem for two values of $N=32$ and $N=64$. The thin red dot–dashed line represents the linear fit at slow rates $n_b/N\approx 0.057\lambda$ and the numerical data approach this asymptotic in an $N$-independent manner.

Thus the number of remaining bosons, a measure of deviation of adiabaticity, remains proportional to the rate at slow rates, as opposed to the exponential suppression of the standard Landau-Zener process. Even though one approaches the adiabatic regime when the Landau-Zener parameter is close to 1, the deviation from adiabaticity is still significant and much larger than in the standard problem. This may have significant implications for the experiments such as those reported in Refs. [21,22], provided the initial state is chosen to be atoms and one is interested in the molecule production. We also note that, as far as we can see, this point was not discussed in Ref. [29].

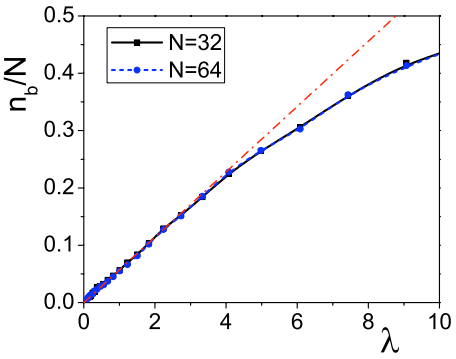


FIG. 15. (Color online) The number of remaining molecules vs λ for the inverse problem, where we start from the full molecular condensate and no atoms. Note that the results for $N=32$ and $N=64$ almost identically coincide. The thin red line represents the linear fit at slow rates: $n_b/N\approx 0.057\lambda$.

In some applications it may be important [17] to explore the sector of the theory where the total number of particles is much smaller than $N$ [i.e., much smaller than the number of two-level systems in Eq. (6) or smaller than the number of fermionic pair levels in Eq. (7)]. Once more, it is easiest to analyze the system in its spin-$N/2$ incarnation (4). Translated to the language of this Hamiltonian a sparse initial occupation of fermionic Hilbert space means that we start the process at zero bosons and a spin that is pointing nearly downward (while the total spin continues to define the dimension of state space, $S=N/2$). The particle conservation law then reads $S_z+n=-N/2+\epsilon$, where $\epsilon\ll N$ and $0\le n\le\epsilon$ is the number of bosons. This regime can be modeled in terms of Holstein-Primakoff bosons. However, as the spin continues to move downward, the regime of Holstein-Primakoff linearizability will not be left. Using

$$S^+ = c^\dagger(2S-c^\dagger c)^{1/2},$$

$$S^- = (2S-c^\dagger c)^{1/2}c,$$

$$S^z = -S+c^\dagger c, \tag{68}$$

where $S=N/2$ [the version of Eq. (11) for the spin pointing close to downward], we find

$$H=\lambda t(b^\dagger b-c^\dagger c)+g(b^\dagger c+c^\dagger b).$$

Here $b^\dagger b+c^\dagger c=\epsilon$. This problem is equivalent to the standard Landau-Zener problem. This proves that in this sector the model reduces to the standard problem and does not have any novel features.

## IX. CONCLUSIONS

Let us summarize the findings of our paper. The model described by Eq. (4) [as well as its other incarnations, given by Eqs. (6)–(8) together with Eq. (10)], with the initial conditions

$$\lim_{t\to-\infty}\langle b^\dagger(t)b(t)\rangle = 0,$$

results in a total final number of bosons $n_b$ defined by

$$n_b = \lim_{t\to+\infty}\langle b^\dagger(t)b(t)\rangle$$

given by the following expressions:

(i) For small values of the LZ parameter,

$$e^{\pi g^2/\lambda} \ll N: \quad n_b = e^{\pi g^2/\lambda} - 1.$$

This result can be obtained within the Holstein-Primakoff method, or by the large-$N$ approximation within the Keldysh formalism.

(ii) At intermediate values,

$$e^{\pi g^2/\lambda} \simeq N: \quad n_b \simeq \frac{N(e^{\pi g^2/\lambda}-1)}{2e^{\pi g^2/\lambda}+N}.$$

This can be found using the kinetic equation approach within the Keldysh formalism.

(iii) At large values,

$$e^{\pi g^2/\lambda} \gg N: \quad n_b \simeq N\left(1-\frac{\lambda}{\pi g^2}\ln(N)\right).$$

This result was found using the quasiclassical approximation together with the adiabatic invariants formalism. We observe main distinctions between our results and what would have happened had we extrapolated the standard Landau-Zener to our problem [which would have given $n_b=N(1-e^{-\pi g^2/\lambda})$]. First, the transition between the fast rate and slow rate regimes happens at

$$\lambda \simeq \frac{\pi g^2}{\ln N},$$

the rate which becomes progressively smaller as $N$ is increased (unlike the Landau-Zener result $\lambda \simeq \pi g^2$). Second, if $\lambda \ll \pi g^2/\ln N$, then $n_b$ approaches $N$ as a linear function of $\lambda$, much more slowly than the Landau-Zener result which would predict an exponentially fast approach. Finally, particle occupancies in our system show massive quantum fluctuations, comparable in value to the mean particle numbers.

*Note added.* Recently, a preprint Ref. [47] appeared which confirmed and further extended our results in the deep adiabatic regime.

## ACKNOWLEDGMENTS

A.A. acknowledges discussions with Fritz Haake. This work was supported by SFB/TR 12 of the Deutsche Forschungsgemeinschaft, by the NSF Grant No. DMR-0449521, and by AFOSR YIP.

## APPENDIX A: DERIVATION OF EQS. (13) and (14)

Consider the Heisenberg equations of motion $i\partial_t x = [\hat{H},x]$, $x=c,b$ corresponding to the Hamiltonian (12),

$$i\partial_t b + \lambda t b + g c^\dagger = 0,$$

$$-i\partial_t c^\dagger + \lambda t c^\dagger + g b = 0. \tag{A1}$$

The structure of these equations suggests the linear combination

$$c = \mu c_0 + \nu b_0^\dagger,$$

$$b = \rho b_0 + \sigma c_0^\dagger, \tag{A2}$$

where $c_0 \equiv c(t_0)$, $t_0 \ll 0$ is some time in the distant past when the dynamical evolution is started, and $\mu,\ldots,\sigma$ are complex-valued functions depending on time. Differentiating the first of the two equations in Eq. (A1) once more with respect to time and substituting the second equation, we obtain

$$[\partial_t^2 - i\lambda + (\lambda t)^2 - g^2]x = 0, \quad x = c,b. \tag{A3}$$

These two equations are coupled by the initial conditions, which follow from the first-order ancestor equations (A1). To make these dependencies explicit, we substitute expansion (A2) and obtain

$$[\partial_t^2 - i\lambda + (\lambda t)^2 - g^2]\kappa = 0, \quad \kappa = \mu,\nu,\rho,\sigma,$$

$$\kappa = \mu,\rho: \quad \kappa(t_0) = 1, \quad \partial_t\kappa(t_0) = i\lambda t_0,$$

$$\kappa = \nu,\sigma: \quad \kappa(t_0) = 0, \quad \partial_t\kappa(t_0) = ig. \tag{A4}$$

Notice that

$$\mu = \rho, \quad \nu = \sigma,$$

$$|\mu|^2 - |\nu|^2 = 1, \tag{A5}$$

where the first line is a consequence of $(\mu,\rho)$ and $(\nu,\sigma)$ obeying differential equations with identical initial conditions and the second is enforced by the fact that the time-dependent operators $(c,c^\dagger,b,b^\dagger)$ obey canonical commutation relations.

These equations afford a solution in terms of parabolic cylinder functions [8]. All we need to know about these functions is that

$$|\mu|^2 \overset{t\to\infty}{\longrightarrow} e^{\pi g^2/\lambda}. \tag{A6}$$

Using $n_b = \langle c^\dagger c\rangle = \langle(\bar{\mu}c_0^\dagger + \bar{\nu}b_0)(\mu c_0 + \nu b_0^\dagger)\rangle = |\nu|^2$ and Eqs. (A5) and (A6) we then obtain Eq. (13).

The actual distribution of the particle number can be obtained by a bit of linear algebra. We begin by condensing Eq. (A2) into the matrix equation

$$\begin{pmatrix} c \\ b^\dagger \end{pmatrix} = \begin{pmatrix} \mu & \nu \\ \bar{\nu} & \bar{\mu} \end{pmatrix}\begin{pmatrix} c_0 \\ b_0^\dagger \end{pmatrix} \Rightarrow \begin{pmatrix} c_0 \\ b_0^\dagger \end{pmatrix} = \begin{pmatrix} \bar{\mu} & -\nu \\ -\bar{\nu} & \mu \end{pmatrix}\begin{pmatrix} c \\ b^\dagger \end{pmatrix}, \tag{A7}$$

where we used Eq. (A5). Denoting the occupation number eigenstates of the time-dependent operators by $|k,l\rangle$, i.e.,

$$c|k,l\rangle = \sqrt{k}|k-1,l\rangle, \quad c^\dagger|k,l\rangle = \sqrt{k+1}|k+1,l\rangle,$$

$$b|k,l\rangle = \sqrt{l}|k,l-1\rangle, \quad b^\dagger|k,l\rangle = \sqrt{l+1}|k,l+1\rangle.$$

We now expand the vacuum state (of the operators $c_0$ and $b_0$) $|0\rangle$ in the basis $\{|k,l\rangle\}$ as follows:

$$|0\rangle = \sum_{k,l} c_{k,l}|k,l\rangle.$$

To determine the coefficients $c_{k,l}$, we use the defining relation

$$0 \stackrel{!}{=} c_0|0\rangle$$

$$= (\bar{\mu}c - \nu b^\dagger)\sum_{k,l} c_{k,l}|k,l\rangle \quad \text{[through (A7)]}.$$

This equation and its partner $b_0|0\rangle=0$ generate the set of recursion relations

$$c_0|0\rangle = 0: \quad \mu\sqrt{k+1}c_{k+1,l+1} = \bar{\nu}\sqrt{l+1}c_{k,l}, \quad k,l \geq 0,$$

$$\mu c_{k,0} = 0, \quad k \geq 1,$$

$$b_0|0\rangle = 0: \quad \bar{\nu}\sqrt{k+1}c_{k,l} = \mu\sqrt{l+1}c_{k+1,l+1}, \quad k,l \geq 0,$$

$$\mu c_{0,l} = 0, l \geq 1.$$

From these equations we deduce $c_{k,0}=0$ for $k\geq 0$ and $c_{0,l}=0$ for $l\geq 0$ (however, $c_{0,0}$ is not zero). The first and third equations then imply $c_{k,l}=0$ for $k\neq l$. The diagonal terms successively descend from $c_{0,0}$ according to

$$c_{k,l} = \delta_{k,l}c_{0,0}\left(\frac{\bar{\nu}}{\mu}\right)^k.$$

The normalization condition $1=\langle 0|0\rangle=\Sigma_{k,l}|c_{k,l}|^2$ generates the additional condition

$$1 = \frac{|c_{0,0}|^2}{1-\left|\frac{\bar{\nu}}{\mu}\right|^2} = |c_{0,0}|^2|\mu|^2.$$

We thus arrive at the expansion

$$|0\rangle = \frac{1}{|\mu|}\sum_{k=0}^{\infty}\left(\frac{\bar{\nu}}{\mu}\right)^k|k,k\rangle.$$

From this, the moments of the particle number operator are straightforwardly obtained as

$$c_m \equiv \langle 0|(c^\dagger c)^m|0\rangle = \frac{1}{|\mu|^2}\sum_{k=0}^{\infty}\frac{|\nu|^{2k}}{|\mu|^{2k}}k^m.$$

Comparison with the formulation of moments in terms of the discrete probability distribution $P(n)$

$$c_m = \sum_n P(n)n^m$$

leads to the identification $P(n)=\frac{1}{|\mu|^2}\frac{|\nu|^{2n}}{|\mu|^{2n}}$ or, using Eq. (A5),

$$P(n) = \frac{1}{|\mu|^2}\left(1-\frac{1}{|\mu|^2}\right)^n. \tag{A8}$$

Substitution of Eq. (A6) then leads to Eq. (14). From this distribution, the mean value is readily obtained as Eq. (13).

## APPENDIX B: DERIVATION OF THE TRUNCATED WIGNER APPROXIMATION FOR THE SPIN-BOSON MODEL

### 1. Truncated Wigner approximation

In this appendix, we first review the TWA for a general system of bosons and then adapt to our specific spin-boson problem. Consider a (generally time-dependent) Hamiltonian formulated in terms of normal ordered bosonic creation and annihilation operators $\mathcal{H}(\hat{\psi}^\dagger,\hat{\psi},t)$. The hat notation $\hat{\psi}$ is used to distinguish operators from $c$ numbers. In the classical limit the operators $\hat{\psi}$ are substituted by complex numbers $\psi$ satisfying the Hamiltonian equation of motion (Gross-Pitaevskii equation)

$$i\hbar\frac{\partial\psi}{\partial t} = \frac{\delta\mathcal{H}(\psi^*,\psi,t)}{\delta\psi^*},$$

where the right-hand side denotes a variational derivative. Classically, these equations have to be supplied by definite initial conditions $(\psi_0,\psi_0^*)$. Within the truncated Wigner approximation—the first-order quantum correction to the classical picture—the initial data becomes a distribution $W(\psi_0,\psi_0^*)d\psi_0 d\psi_0^*$. The kernel of this distribution is defined by

$$W_0(\psi_0,\psi_0^*) = \int d\eta_0^* d\eta_0 \left\langle \psi_0 - \frac{\eta_0}{2}\middle|\rho\middle|\psi_0+\frac{\eta_0}{2}\right\rangle \times e^{-|\psi_0|^2-(1/4)|\eta_0|^2}e^{(1/2)(\eta_0^*\psi_0-\eta_0\psi_0^*)}, \tag{B1}$$

where $\rho$ is the initial density matrix of the system. Expectation values of operators $\Omega(\hat{\psi}^\dagger,\hat{\psi})$ at time $t$ are then to be calculated as [32]

$$\langle\Omega(t)\rangle = \int\int d\psi_0 d\psi_0^*\, W_0(\psi_0,\psi_0^*)\Omega_{cl}(\psi(t),\psi^*(t)), \tag{B2}$$

where $\psi(t)$ is the solution of the classical Gross-Pitaevskii equations of motion with initial condition $\psi_0$ and $\Omega_{cl}(\psi,\psi^*)$ is the Weyl symbol of the operator $\Omega$. For a normal ordered $\Omega$ the latter is defined by

$$\Omega_{cl}(\psi,\psi^*) = \int\int d\eta d\eta^*\, \Omega(\psi-\eta/2,\psi^*+\eta^*/2)e^{-|\eta|^2/2}, \tag{B3}$$

where $\Omega(\psi,\psi^*)$ is obtained by substitution of operators in $\Omega(\hat{\psi},\hat{\psi}^\dagger)$ as $\hat{\psi}\to\psi$ and $\hat{\psi}^\dagger\to\psi^*$. For example for the number operator $\Omega=\hat{\psi}^\dagger\hat{\psi}$ we get

$$\Omega_{cl} = \int\int d\eta d\eta^*(\psi - \eta/2)(\psi^* + \eta^*/2)e^{-|\eta|^2/2} = \psi^*\psi - \frac{1}{2}. \tag{B4}$$

The same result can be obtained by first symmetrizing number operator with respect to $\hat{\psi}^\dagger$ and $\hat{\psi}$, i.e.,

$$\hat{\psi}^\dagger\hat{\psi} = \frac{\hat{\psi}^\dagger\hat{\psi} + \hat{\psi}\hat{\psi}^\dagger}{2} - \frac{1}{2} \tag{B5}$$

and then substituting the operators $\hat{\psi}^\dagger$ and $\hat{\psi}$ with the numbers $\psi^*$ and $\psi$ (see Ref. [36]) for more details.

### 2. Adaptation to the spin-boson problem

Our next task is to generalize the TWA to the Hamiltonian (4). To this end, we employ the Schwinger representation of spins through bosons $\hat{\alpha}$ and $\hat{\beta}$ as follows:

$$\hat{S}^z = \frac{\hat{\alpha}^\dagger\hat{\alpha} - \hat{\beta}^\dagger\hat{\beta}}{2}, \quad \hat{S}^+ = \hat{\alpha}^\dagger\hat{\beta}, \quad \hat{S}^- = \hat{\beta}^\dagger\hat{\alpha}. \tag{B6}$$

Here, the boson operators $\alpha$ and $\beta$ satisfy the additional constraint $\hat{n} = \hat{\alpha}^\dagger\hat{\alpha} + \hat{\beta}^\dagger\hat{\beta} = 2S$. The operator $\hat{n}$ commutes with all spin operators which means that the fulfillment of the constraint at an arbitrary time will be conserved for all later times. The option of a purely bosonic representation means that the TWA can readily be generalized to the Hamiltonian (4). Once the TWA has been formulated for the Schwinger bosons, we are at liberty to switch back to spin variables (B6). However, at this point, the spins have become classical numbers, defined in terms of the $c$-number-valued boson variables $\alpha$ and $\beta$.

The classical equations of motion are given by Eq. (33). The initial density matrix describes a pure spin state, polarized along the $z$ axis or, in bosonic language, a state with $2S$ $\alpha$ bosons and no $\beta$ bosons. (For the spin pointing along $-z$ $\alpha$ and $\beta$ should be interchanged.) The corresponding Wigner function then reads [32,33,48]

$$W(\alpha,\alpha^*,\beta,\beta^*) = 2e^{-2|\alpha|^2-2|\beta|^2}L_{2S}(4|\alpha|^2), \tag{B7}$$

where $L_N(x)$ is the Laguerre polynomial of order $N$. At large $S$, the latter is strongly oscillatory and the Wigner transform is localized near $|\alpha|^2 = 2S + 1/2$ (see Ref. [32]). So in this case to a very good accuracy (up to $1/S^2$) one can use

$$W(\alpha,\alpha^*,\beta,\beta^*) \approx \sqrt{2}e^{-2|\beta|^2}\delta(|\alpha|^2 - 2S - 1/2). \tag{B8}$$

If we re-express this distribution function through spins then to the same accuracy we will find

$$W(S_z,S_\perp) \approx \frac{1}{\pi S}e^{-S_\perp^2/S}\delta(S_z - S),$$

where $S_\perp^2 = S_x^2 + S_y^2$. This Wigner function has a transparent interpretation. If the quantum spin points along the $z$ direction, because of the uncertainty principle, the transverse spin components still experience quantum fluctuations, so that

$$\langle S_x^2\rangle = \langle S_y^2\rangle = \frac{S}{2},$$

which is indeed the correct quantum-mechanical result. Finally, the distribution of the $b$ boson represents the Gaussian Wigner function of the vacuum state,

$$W(b,b^*) = 2\exp[-2b^*b] \equiv W(n) = 2\exp[-2n],$$

where in the second representation we switched to a representation in terms of the boson number $n = b^*b$.

### 3. TWA versus quantum solution of linear regime

We here discuss how the solution of the equations of motion (36) obtains information equivalent to that of the full quantum solution of the linear regime. To this end, we notice that the equations afford a solution as [see Eq. (A2)]

$$b(t) = \mu b(t_0) + \nu s^-(t_0), \quad s^-(t) = \mu^* s^-(t_0) + \nu^* b(t_0),$$

where at $t \to \infty$ we have $|\mu|^2 = x$ and $|\nu^2| = x - 1$ [see Eqs. (A5) and (A6)]. If we are interested only in the statistics of the number of bosons we do not need to know the phases of $\mu$ and $\nu$. Using the Wigner function (B1) to compute the average and the Weyl symbol (35) for the operators $n_b$ and $n_b^2$ it is then straightforward to obtain

$$\langle n_b\rangle = x\langle n_b(t_0)\rangle + (x-1)\langle|s^-(t_0)|^2\rangle - \frac{1}{2} = x - 1$$

and the second moment

$$\langle n_b^2\rangle = -x + \frac{1}{2} + x^2\langle n_b^2(t_0)\rangle + (x-1)^2\langle|s^-(t_0)|^4\rangle + 4x(x-1)$$
$$\times\langle n_b(t_0)\rangle\langle|s^-(t_0)|^2\rangle = 2x^2 - 3x + 1.$$

It is easy to check that this result conforms to distribution (14).

## APPENDIX C: MEANING OF THE FIXED POINTS

Let us consider the time-independent version of the model studied in this paper. It is given by the time-independent version of the Hamiltonian (4)

$$\hat{H} = -\frac{\gamma}{2}b^\dagger b + \frac{\gamma}{2}S^z + \frac{1}{\sqrt{N}}(b^\dagger S^- + bS^+), \tag{C1}$$

where $g$ has been scaled to 1. In the sector where

$$b^\dagger b + S^z = \frac{N}{2},$$

which is the one mostly studied in this paper, this Hamiltonian can be thought of as simply a $(N+1)\times(N+1)$ matrix. In the basis of states $|n\rangle$ where $n$ denotes the boson occupation number, this matrix takes the form

$$H_{n',n} = -\gamma n\delta_{n',n} + \frac{1}{\sqrt{N}}n\sqrt{N-n'}\,\delta_{n'+1,n} + \frac{1}{\sqrt{N}}n'\sqrt{N-n}\,\delta_{n'-1,n} \tag{C2}$$

[compare with Eq. (9)]. It is easy to evaluate the eigenvalues of this matrix numerically for moderate $N$.

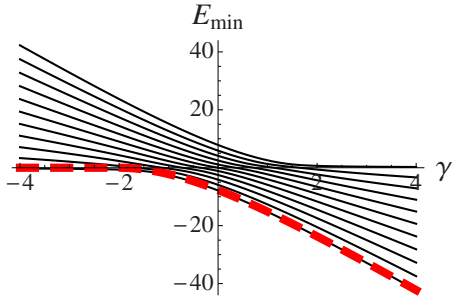


FIG. 16. (Color online) The energy levels [eigenvalues of the matrix Eq. (C2)] for $N=10$ are plotted as a function of $\gamma$. At the same time, the minimum of the classical Hamiltonian, given by Eq. (C3), is also plotted (dashed red curve). We see that Eq. (C3) closely follows the ground-state energy of Eq. (C2).

Now consider a semiclassical version of this Hamiltonian [Eq. (41)] which for completeness we reproduce here

$$H = -\gamma n - 2n\sqrt{1-n}\cos(\phi).$$

Here both the Hamiltonian and the variable $n$ were rescaled according to Eqs. (39) and (40) to ease comparison with the language of Sec. VI, although we need to keep that in mind when comparing it with Eq. (C2) which was not rescaled in any way. Let us minimize this Hamiltonian with respect to $n$ and $\phi$. Its minimum is given by the substitution of the fixed point $\phi=0$, and $n_1(\gamma)$ given by $n_1(\gamma)=0$ for $\gamma<-2$ and by Eq. (44), or

$$n_1(\gamma) = \frac{12-\gamma^2+\gamma\sqrt{12+\gamma^2}}{18}$$

if $\gamma \geq -2$. To find the energy minimum we substitute $n_1(\gamma)$ into $H$ to find

$$E_{\min} = N \min_{n,\phi} H = 0, \quad \text{if} \quad \gamma < -2$$

$$E_{\min} = -N\frac{36\gamma-\gamma^3+(12+\gamma^2)^{3/2}}{54} \quad \text{if} \quad \gamma \geq -2. \tag{C3}$$

The minimum of the classical Hamiltonian (C3), together with the eigenvalues of Eq. (C2), is plotted as a function of $\gamma$ on Fig. 16 for $N=10$. One can see that the classical minimum closely follows the quantum ground state. Yet Eq. (C3) cannot be the exact ground state of the problem at this value of $N$ since it is not analytical in $\gamma$. However, it can be the exact ground state in the limit $N\to\infty$. Thus we conjecture that Eq. (C3) *is* the ground state of the Hamiltonian in our problem in the limit $N\to\infty$. If so, it implies that our problem undergoes a quantum phase transition as a function of $\gamma$.

When $\gamma$ depends on time, it follows that we drive our system across the quantum phase transition. The existence of the critical trajectory and the singular behavior of the adiabatic invariants discussed in Sec. VI can be traced to the existence of this transition. The transition in the time-independent version of the Dicke model is well known in the literature (see, for example, Ref. [49] and references therein).

## APPENDIX D: DERIVATION OF EQ. (62)

Here, just as in Sec. VI, we use the rescaled variables $n$ and $H$, according to Eqs. (39) and (40). To obtain the value of $\epsilon=\epsilon^*$ at which $w=\pi$, we need to inspect the increment of the angular variable $w$ in the problem where $\gamma$ changes in time. It satisfies the equation [37]

$$d_t w = \omega + \left(\frac{\partial\Lambda}{\partial I}\right)_{w,\gamma}\lambda,$$

where $\Lambda$ was defined in Eq. (53). At small $\lambda$ we neglect the second term to arrive at

$$w(\epsilon) \approx \int_{\epsilon_0}^{\epsilon} d\epsilon' \frac{\pi\sqrt{\epsilon'}}{\lambda \ln\left[-\frac{16\epsilon'^2}{H}\right]}. \tag{D1}$$

Here we used Eq. (58), the identity $d\epsilon/dt=2\lambda$, and $\epsilon_0>0$ denotes the moment of time when the system crosses the critical trajectory and switches to trajectories winding about the critical point (45). This allows us to find $w$ as a function of $\epsilon$, which in turn represents time. To compute this integral, we need to know $H(\epsilon)$. This in turn can be estimated by noting that

$$d_t H = -2\lambda n.$$

Here, $n$ itself is a function of time, which satisfies its equation of motion $d_t n=-2n\phi$. Using Eq. (60) we find

$$n = n_0 \exp\left(-\frac{1}{\lambda}\int_{\epsilon_0}^{\epsilon} d\epsilon' \phi\right) = n_0 e^{(2/3\lambda)(\epsilon^{3/2}-\epsilon_0^{3/2})}, \tag{D2}$$

which integrates to

$$H = -n_0 \int_{\epsilon_0}^{\epsilon} d\epsilon' \, e^{(2/3\lambda)(\epsilon'^{3/2}-\epsilon_0^{3/2})}. \tag{D3}$$

This needs to be substituted into Eq. (D1). We are now in a position to estimate the value $\epsilon^*$ corresponding to $w=\pi$. To compute the integrals in Eq. (D1), we need to study the behavior of $H$. At small $\epsilon-\epsilon_0$, $H$ can be approximated as

$$H \approx -n_0(\epsilon-\epsilon_0).$$

At larger $\epsilon$, we can estimate it by

$$H \approx -n_0\frac{\lambda}{\sqrt{\epsilon}}e^{(2/3\lambda)\epsilon^{3/2}}.$$

Here, $\epsilon_0$ represents the moment in time when the system crosses the critical trajectory. At this point $n$ did not have a chance to change appreciably from its initial value, $n(\gamma\to-\infty)$. Thus $n_0\sim\frac{1}{N}$. This means that to logarithmic accuracy, we may use the approximation $H(\epsilon)\sim -1/N$ in Eq. (D1). Other factors, such as $16\epsilon^2$ under the logarithm can also be neglected. This leads to

$$w = \int_{\epsilon_0}^{\epsilon^*} d\epsilon \frac{\pi\sqrt{\epsilon}}{\lambda \ln[N]} \sim \frac{2\epsilon^{*\,3/2}}{3\lambda \ln N} \overset{!}{\sim} \pi.$$

Solution of this equation for $\epsilon^*$ obtains result (62). Our derivation has been self-consistent in the sense that even at the maximal value $\epsilon^*$,

$$|H(\epsilon^*)| \sim \frac{\lambda^{1/3}}{\left(\frac{3}{2}\ln N\right)^{2/3}} \ll \epsilon^{*2},$$

where again the conditions (37) were used.

The last thing which remains to be done is to check that Eq. (60) is consistent with the behavior of the system. The equation of motion (59), together with the condition that $|H| \ll \epsilon^2$, implies

$$2\lambda d_\epsilon \phi = -\epsilon + \phi^2,$$

assuming that $\phi^2 \leq \epsilon$. This is a Riccati equation, which can be brought to the form of the Schrödinger equation by the substitution

$$R = \exp^{(-1/2\lambda \int \phi d\epsilon)}$$

to give

$$-2\lambda \frac{d^2R}{d\epsilon^2} + \epsilon R = 0.$$

This is the equation for the Airy function. It can be investigated using the WKB approximation, which reproduces the ansatz $\phi = -\sqrt{\epsilon}$. Close to $\epsilon = 0$, the WKB approximation breaks down, so this ansatz is no longer correct. However, it is easy to modify relations such as Eq. (D2) and (D3) by substituting $R^2$, with $R$ being the appropriate Airy function, in place of the exponentials in these relations. This does not affect the final answer for $\epsilon^*$, and consequently for $I_{\text{final}}$.


[1] L. Landau, Phys. Z. Sowjetunion **2**, 46 (1932).
[2] C. Zener, Proc. R. Soc. London, Ser. A **137**, 696 (1932).
[3] Y. N. Demkov, Sov. Phys. Dokl. **11**, 138 (1966).
[4] V. I. Osherov, Sov. Phys. JETP **22**, 804 (1966).
[5] Y. Kayanuma and S. Fukichi, J. Phys. B **18**, 4089 (1985).
[6] S. Brundobler and V. Elser, J. Phys. A **26**, 1211 (1993).
[7] V. A. Yurovsky, A. Ben-Reuven, and P. S. Julienne, Phys. Rev. A **65**, 043607 (2002).
[8] M. A. Kayali and N. A. Sinitsyn, Phys. Rev. A **67**, 045603 (2003).
[9] B. Wu and Q. Niu, Phys. Rev. A **61**, 023402 (2000).
[10] J. Liu, L. Fu, B. Y. Ou, S. G. Chen, D. I. Choi, B. Wu, and Q. Niu, Phys. Rev. A **66**, 023404 (2002).
[11] O. Zobay and B. M. Garraway, Phys. Rev. A **61**, 033603 (2000).
[12] A. Altland and V. Gurarie, Phys. Rev. Lett. **100**, 063602 (2008).
[13] I. Tikhonenkov, E. Pazy, Y. B. Band, M. Fleischhauer, and A. Vardi, Phys. Rev. A **73**, 043605 (2006).
[14] E. Bertin and M. Clusel, J. Phys. A **39**, 7607 (2006).
[15] C. A. Regal, M. Greiner, and D. S. Jin, Phys. Rev. Lett. **92**, 040403 (2004).
[16] M. W. Zwierlein, C. A. Stan, C. H. Schunck, S. M. F. Raupach, A. J. Kerman, and W. Ketterle, Phys. Rev. Lett. **92**, 120403 (2004).
[17] D. Sun, A. Abanov, and V. Pokrovsky, EPL **83**, 16003 (2008).
[18] R. H. Dicke, Phys. Rev. **93**, 99 (1954).
[19] E. M. Chudnovsky and D. A. Garanin, Phys. Rev. Lett. **89**, 157201 (2002).
[20] J. M. Raimond, M. Brune, and S. Haroche, Rev. Mod. Phys. **73**, 565 (2001).
[21] E. Hodby, S. T. Thompson, C. A. Regal, M. Greiner, A. C. Wilson, D. S. Jin, E. A. Cornell, and C. E. Wieman, Phys. Rev. Lett. **94**, 120402 (2005).
[22] S. B. Papp and C. E. Wieman, Phys. Rev. Lett. **97**, 180404 (2006).
[23] E. Altman and A. Vishwanath, Phys. Rev. Lett. **95**, 110404 (2005).
[24] R. Barankov and L. Levitov, e-print arXiv:cond-mat/0506323.
[25] B. E. Dobrescu and V. L. Pokrovsky, Phys. Lett. A **350**, 154 (2006).
[26] J. von Stecher and C. H. Greene, Phys. Rev. Lett. **99**, 090402 (2007).
[27] L. Radzihovsky, J. Park, and P. B. Weichman, Phys. Rev. Lett. **92**, 160402 (2004).
[28] M. J. Ablowitz, B. A. Funk, and A. C. Newell, Stud. Appl. Math. **52**, 51 (1973).
[29] J. Liu, B. Liu, and L. B. Fu, Phys. Rev. A **78**, 013618 (2008).
[30] R. Schützhold, Phys. Rev. Lett. **95**, 135703 (2005).
[31] A. Kamenev, *Nanophysics: Coherence and Transport*, Les Houches 2004 Session No. 81 (Elsevier, Amsterdam, 2005); e-print arXiv:cond-mat/0412296.
[32] A. Polkovnikov, Phys. Rev. A **68**, 053604 (2003).
[33] D. Walls and G. Milburn, *Quantum Optics* (Springer-Verlag, Berlin, 1994).
[34] C. Gardiner and P. Zoller, *Quantum Noise*, 3rd ed. (Springer-Verlag, Berlin, 2004).
[35] M. J. Steel, M. K. Olsen, L. I. Plimak, P. D. Drummond, S. M. Tan, M. J. Collett, D. F. Walls, and R. Graham, Phys. Rev. A **58**, 4824 (1998).
[36] P. B. Blakie, A. S. Bradley, M. J. Davis, R. J. Ballagh, and C. W. Gardiner, Adv. Phys. **57**, 363 (2008)
[37] L. D. Landau and E. M. Lifshitz, *Mechanics* (Butterworth-Heinemann, Oxford, UK, 1982).
[38] V. Gritsev, E. Altman, E. Demler, and A. Polkovnikov, Nat. Phys. **2**, 705 (2006).
[39] A. Polkovnikov and V. Gritsev, Nat. Phys. **4**, 477 (2008).
[40] A. Polkovnikov, Phys. Rev. B **72**, 161201(R) (2005).
[41] W. H. Zurek, U. Dorner, and P. Zoller, Phys. Rev. Lett. **95**, 105701 (2005).
[42] J. Dziarmaga, Phys. Rev. Lett. **95**, 245701 (2005).
[43] K. Sengupta, D. Sen, and S. Mondal, Phys. Rev. Lett. **100**, 077204 (2008).
[44] S. Mondal, D. Sen, and K. Sengupta, Phys. Rev. B **78**, 045101 (2008).
[45] V. Mukherjee, U. Divakaran, A. Dutta, and D. Sen, Phys. Rev. B **76**, 174303 (2007).
[46] T. Caneva, R. Fazio, and G. E. Santoro, Phys. Rev. B **76**, 144427 (2007).
[47] A. P. Itin and P. Törmä, e-print arXiv:0901.4778.
[48] A. Polkovnikov, Phys. Rev. A **68**, 033609 (2003).
[49] F. Dimer, B. Estienne, A. S. Parkins, and H. J. Carmichael, Phys. Rev. A **75**, 013804 (2007).
[50] A V. Shytov, Phys. Rev. A **70**, 052708 (2004).